POLYTECHNIQUE MONTRÉAL

affiliée à l'Université de Montréal

Finite Element Model to Investigate the Dynamic Instability of a Rectangular Plate Subjected to Supersonic Airflow

HOSSEIN BAHRAMI TORABI

Département de génie mécanique

Mémoire présenté en vue de l'obtention du diplôme de *Maîtrise ès sciences appliquées*

Génie mécanique

Décembre 2020

© Hossein Bahrami Torabi, 2020.

POLYTECHNIQUE MONTRÉAL

affiliée à l'Université de Montréal

Ce mémoire intitulé :

Finite Element Model to Investigate the Dynamic Instability of a Rectangular Plate Subjected to Supersonic Airflow

présenté par **Hossein BAHRAMI TORABI**

en vue de l'obtention du diplôme de *Maîtrise ès sciences appliquées*

a été dûment accepté par le jury d'examen constitué de :

Aboulfazl SHIRAZI-ADL, président
Aouni LAKIS, membre et directeur de recherche
Abdelhak OULMANE, membre

DEDICATION

I dedicate my dissertation work to my family. Also, I dedicate this dissertation to the memory of my beloved grandfather, Javad Bahrami Torabi, who passed away while I was a sophomore student at Polytechnique Montreal.

ACKNOWLEDGEMENTS

I would like to express my sincere appreciation to my supervisor, Professor Aouni Lakis, and co-supervisor, Professor Youcef Kerboua, whose assistance was a milestone in the completion of this project. I also wish to acknowledge the support of my family, and my wife, Nafiseh. They supported me a lot and without their help, this work would not have been possible to accomplish.

RÉSUMÉ

Dans cette thèse, une méthode numérique est présentée pour étudier le comportement dynamique d'une plaque rectangulaire isotrope soumise à des charges aérodynamiques induites par un flux d'air supersonique parallèle. Un modèle d'éléments finis, basé sur des fonctions de déplacement polynomiales bidimensionnelles et sur la théorie des pistons linéaires, est utilisé pour étudier le comportement dynamique de la plaque solide couplée avec charges aérodynamiques. L'approche développée est capable de modéliser des plaques plates et des coques peu profondes dans lesquelles le couplage fluide-structure à l'interface est appliqué de manière synchrone sur la base d'une méthode monolithique. La raideur élémentaire et l'amortissement obtenus à partir de la charge aérodynamique sont couplés avec à ceux obtenus à partir du modèle structurel et ils sont calculés par intégration analytique. En assemblant les matrices élémentaires, nous obtenons les matrices globales de masse, d'amortissement et de raideur de notre plaque puis nous pouvons écrire les équations dynamiques régissant notre problème. Les valeurs propres du système sont calculées selon la méthode réduite. La pression aérodynamique non dimensionnelle critique du flux d'air induisant le flottement de la structure est déterminée pour diverses conditions aux limites et géométries. Les résultats obtenus sont comparés aux travaux de recherche publiés et un très bon accord a été souligné.

ABSTRACT

In this thesis, a numerical method is presented to study the dynamic behaviour of an isotropic rectangular plate subjected to aerodynamic loads induced by parallel supersonic airflow. A finite element model, based on bi-dimensional polynomial displacement functions and linear Piston theory, is used to study the dynamic behaviour of the solid plate coupled with aerodynamic loads. The developed approach is capable to model flat plates and shallow shells in which the fluid-structure coupling at the interface is applied synchronously based on a monolithic method. The stiffness and damping obtained from aerodynamic load are coupled with those obtained from structural model and they are calculated using analytical integration. By assembling the matrices, we obtain the global mass, damping and stiffness matrices for our plate and then we can write the dynamic equations governing our problem. The eigenvalues of the system are calculated using reduced method. The critical non-dimensional aerodynamic pressure of the airflow inducing flutter of the structure is determined for various boundary conditions and geometries. The obtained results are compared with the published research works and a very good agreement is obtained.

TABLE OF CONTENTS

LIST OF TABLES

LIST OF FIGURES

LIST OF SYMBOLS AND ABBREVIATIONS

A, B	Plate side length in $X$and Ydirections, respectively
$[A]$	Matrix (24 × 24) defined by Eq. (7)
$[B]$	Matrix (24 × 24) defined by Eq. (11)
C_j	Constants defined by Eq. (1), Eq. (2) and Eq. (3)
$\{C\}$	Vector of unknown constants defined by Eq. (4)
$[c_a]$	Aerodynamic damping matrix of an element (24 × 24)
D	Membrane rigidity $Eh/12(1-\nu^2)$
E	Modulus of elasticity
$\{F_a\}^e$	Elementary aerodynamic load vector
h	Plate thickness
i	Complex number $i^2=-1$
$[k_a]$	Aerodynamic stiffness matrix of an element (24 × 24)
$[k]^e$	Stiffness matrix of an element (24 × 24)
K	Bending rigidity $Eh^3/12(1-\nu^2)$
$[m]^e$	Mass matrix of an element (24 × 24)
M_∞	Mach number
$[N]$	Shape function matrix (3 × 24) defined by Eq. (9)
$[P]$	Elasticity matrix (6 × 6)
P	Pressure equation for piston theory
$[Q]$	Matrix (6 × 24) defined by Eq. (11)
Q_∞	Dynamic pressure
$[R]$	Matrix (3 × 24) defined by Eq. (4)

U, V	In-plane displacement in X and Y directions, respectively
U_i, V_i	Nodal displacement components at node $i$in X and Y directions, respectively
V_∞	Free stream velocity
W	Transverse displacement in Z direction
W_i	Transverse displacement in Z direction at node i
x_e, y_e	Length of the element along the X and Yaxes, respectively
XYZ	Orthogonal coordinate system
β	Constant$\sqrt{{M_\infty}^2 - 1}$
$\{\delta\}$	Nodal displacement vector defined by Eq. (5)
δ_G	Global displacement vector of the plate
$\{\varepsilon\}$	Deformation vector
λ	Dimensionless dynamic pressure $2Q_\infty A^3/\beta K$
ν	Poisson's coefficient
ρ	Material density
$\{\sigma\}$	Stress vector
ω	Natural frequency of the plate in rad/s
ANCF	Absolute nodal coordinate formulation
AEM	Analog equation method
AMM	Assumed mode method
BEM	Boundary element method
EPT	Enhanced piston theory
FG	Functionally graded
FSI	Fluid-solid interaction

FEM	Finite element method
LCO	Limit cycle oscillation
POD	Proper orthogonal decomposition

LIST OF APPENDICES

CHAPTER 1 INTRODUCTION

Aeroelasticity is considered a branch of applied mechanics, which is concerned about the motion of a deformable body through an airstream. The origin of Aeroelasticity comes from aircraft engineering, where aeroelastic problems turned out to be important since the beginning of the powered flight. The aeroelasticity gaining more importance in other branches of engineering, as well. There is a general trend to build larger and thus more elastic structures and components in civil engineering, turbomachinery, and hydraulic plants, where aero- and hydro-elastic phenomena appear increasingly more often as limiting factors. From this, it is apparent that the field of aeroelasticity is still in expansion.

Static aeroelasticity is defined as the study of interaction between the steady flow aerodynamics and the static solid mechanics phenomena [1]. Divergence and control reversal are two major phenomena considered in the static aeroelasticity [2]. When a lifting surface is under an aerodynamic load, the structure deflects, and if the deflection continues, the aerodynamic load increases until the divergence point (i.e., the failure point of the structure). When there is a lack of response in a control surface, control reversal occurs, and the reason is deformation of the lifting surface [2].

Dynamic aeroelasticity is defined as the interaction of an elastic body with aerodynamic and inertial forces. Flutter is an extreme and dangerous phenomenon encountered in flexible structures subjected to aerodynamic forces. This includes aircraft, buildings, telegraph wires, stop signs, and bridges. Flutter is an self-excited vibration with an exponentially increasing amplitude that can destroy a structure as a result of interactions between aerodynamics, stiffness, and inertial forces on a structure [2].

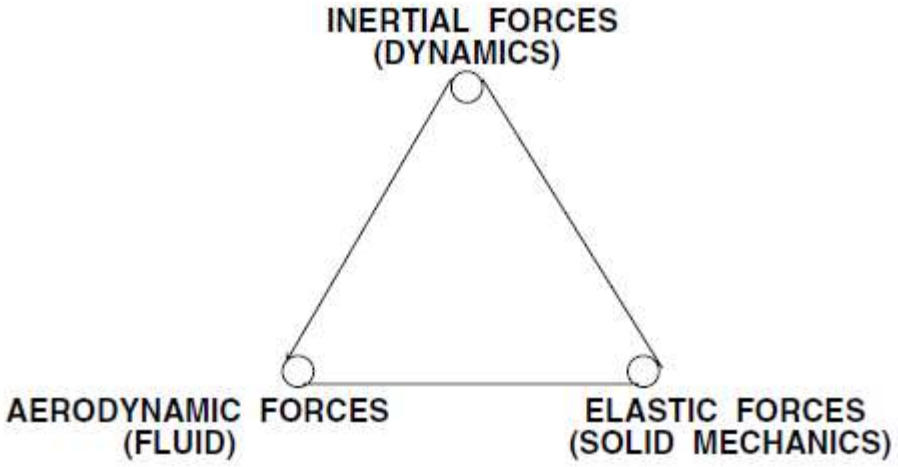

Figure 1: Interaction of inertial forces and structural forces (elastic forces) with aerodynamics [1]

1.1 Literature Review

Plates are commonly used in different industries like aerospace, shipbuilding, and the nuclear industry. The products of all these industrial fields have major economic importance and require a high safety level. Therefore, their dynamic behavior when subjected to external loadings should be well understood to avoid failure.

The combination of aerodynamic, inertial, and elastic forces results in a complex fluid-solid interaction (FSI) problem. Thus, to improve the design and performance of such structures, determining the structure's behavior in response to aeroelastic phenomena is important. For this purpose, either numerical or experimental techniques can be used. However, the experimental methods may face the problem in simultaneous measurement of plate deformations, aerodynamic force, and plate kinematics. To overcome these difficulties, numerical methods or simulations are more attractive.

Major efforts have been devoted by researchers to resolve different issues in this field and a multitude of theoretical [3-17] and experimental works [18-23] have been done during the last decades. Bismark [24] investigated linear flutter of thin plates and underlined that in the hypersonic flight, new mathematical models must be employed in the estimation of aerodynamic loads for analyzing aeroelastic stability of plate and shells. He also mentioned FEM is a robust

method for analyzing complex geometries, materials, and loading; however, it is not still fully applied to different cases and there are limited results to compare with other methods like the Rayleigh–Ritz and Galerkin.

Abbas et al. [25] developed the structural model by using the absolute nodal coordinate formulation (ANCF) procedure to study flutter of a plate subjected to the external supersonic airflow. They took both shear and transversal strains into account in their formulations. A linear piston theory was used to predict the aerodynamic load. The ANCF method was applied to analyze an isotropic plate under different boundary conditions in supersonic flow. They showed that the results obtained by ANCF have good agreement with the results in the literature. Bloomhardt and Dowell [26] worked on the noise reduction of transport aircrafts in the subsonic regime. They used a plate model with a linear potential flow theory to analyze aeroelastic behavior of the wing. They considered two different boundary conditions. First, all edges simply-supported and second, three edges simply supported and one edge (trailing edge) free. They concluded that for a specific boundary condition, with increasing the aspect ratio of the wing, flutter dynamic pressure is increased. Moreover, the flutter dynamic pressure for the case of free trailing edge boundary is higher than the case of all edges simply supported for a fixed aspect ratio. Xie et al. [27] studied nonlinear flutter in supersonic flow for a cantilever plate using the proper orthogonal decomposition (POD) method. They utilized Von Karman plate theory and the first order piston theory in their analysis. They concluded for good convergence, the number of POD modes should be lower than the number of the Rayleigh–Ritz modes and it leaded to less computational efforts. Gibbs and Dowell [28] worked on the stability of rectangular plates in subsonic flow and validated their results with an experimental setup. They considered a linear structural model with an unsteady aerodynamic model to estimate the aerodynamic loads. They used a Rayleigh-Ritz method to solve their numerical problems. They validated their results for a combination of clamped and free boundary conditions to resemble the real wing structure. For each type of boundary conditions, they reported flutter and divergence instabilities in their analysis. Kerboua et al. [29] investigated the linear vibration of a rectangular plate in water. They developed equations of motion using a finite element method and Sanders' shell theory. A polynomial and exponential function were used to model the in-plane and out-of-plane displacement components. Moreover, they used velocity potential and Bernoulli's equation to

determine the fluid load acting on the structure. They compared their results with both experiments and other analytical approaches and a good agreement is found. Katsikadelis and Babouskos [30] studied the flutter response of isotropic thin plates in supersonic flow considering internal and external damping. Governing equations were derived from the classical plate theory and the first order piston theory. The analog equation method (AEM) was employed to decouple foregoing equations into one bi-harmonic as well as two Poisson's equations under fictitious excitation which were solved by employing the boundary element method (BEM). Song and Li [31] investigated the effects of various boundary conditions and the accuracy of assumed mode method (AMM) on the flutter characteristics of an isotropic rectangular plate subjected to a supersonic flow. They employed classical thin plate theory to model structural motion along with piston theory to estimate aerodynamic loads. Equations of motion, derived by Hamilton's principle, were solved using the finite element method and AMM. They found that AMM is not as accurate as finite element method results, and stiffer boundary conditions would substantially improve the stability of the plate. Moreover, when the boundary of the structure is elastically restrained mode veering will occur. Based on Ye and Dowell model [32], Xie et al. [33] extended the work and studied the chaos phenomenon for a cantilever plate in supersonic flow. They showed that with a decreasing length-to-width ratio, the critical dynamic pressure decreases. They employed time histories, phase trajectories, bifurcation diagrams, Poincaré plots, and frequency spectra to identify the evolution of chaos. Xie and Xu [34] focused on the semi-analytical proper orthogonal decomposition methods (S-POD and P-POD methods) and compared their results with the Rayleigh–Ritz and Galerkin methods. They studied both cantilevers and simply supported plates in supersonic flow. They found that the P-POD method is more efficient and accurate than the Galerkin method. Therefore, they recommended using P-POD and S-POD methods for the simply supported and cantilever plate, respectively. Mahran et al. [35] studied a linear isotropic trapezoidal plate wing and explored flutter and divergence using finite element approach. They used the linear vortex lattice method to carry out a divergence analysis and the linear doublet lattice method for flutter analysis. Static condensation was employed to reduce the in-plane degrees of freedom at each node and hence to reduce computation burden. They concluded that by increasing wing taper, divergence, and flutter speeds of the plate increased. Ganji and Dowell [36] studied panel flutter in a two-dimensional

flow using the enhanced piston theory (EPT). They stated that in a specific range of Mach numbers ($1<M<\sqrt{2}$), flutter boundary and post flutter response cannot be determined using the full potential flow theory, because this theory calculates the damping negative and predict the aeroelastic system always unstable. By including higher-order terms of reduced frequency in the solution, the model can accurately predict flutter and post flutter response [37]. They also noted that for $M>\sqrt{2}$ obtained results with the lower order piston theory are near to the results with using enhanced piston theory. Tian et al. [38] considered a trapezoidal wing in hypersonic flow and obtained governing equations using coupled von Karman's large deflection plate theory with the third-order piston theory. They subsequently integrated equations using the Rayleigh-Ritz method along with affine transformation and found that the flutter boundary is substantially affected by increasing the sweep angle at different cord to span ratios. Aravinth et al. [39] studied a trapezoidal wing subjected to parallel flow with different Mach numbers from subsonic to supersonic regimes. They used enhanced piston theory [37] along with von Karman's large deflection plate theory to develop governing equations. They used a Jacobian transformation with the Rayleigh-Ritz approach to convert the cantilever trapezoidal plate into a cantilever square plate to solve nonlinear oscillations of a fluttering plate. They concluded that the amplitude of the limit cycle vibration increases with increasing the dynamic pressure. Moreover, by using EPT fewer modes are necessary to obtain a converged solution and as a consequence computational time will be decreased. Lin et al. [40] investigated the flutter response of an elastic rectangular functionally graded (FG) plate which was reinforced by carbon nanotubes in a hypersonic airflow under aero thermal load. They considered coupled thermo-elastic effects by solving Von-Karman plate theory in conjunction with Fourier's heat conduction equation along with employing the third-order piston theory. They used finite difference and Galerkin methods to solve thermal and aeroelastic equations, respectively. In general, coupled and uncoupled approaches showed relative agreement in buckling, LCO and chaos response but not in motion amplitudes and flutter response.

A finite element model is developed in this thesis to study the dynamic behavior of rectangular plates subjected to parallel supersonic airflow. In the previous works of Lakis et al. [41-42] for axisymmetric structures, displacement fields are used, which offer exact solution of the equilibrium equations. Indeed, the dynamic model of cylindrical shells allows separation of

variables in longitudinal and circumferential directions that make obtaining an exact solution possible. This approach yields a very accurate model and facilitates coupling of fluid-structure equations. However, obtaining exact solutions for equilibrium equations governing rectangular plates is not possible using the same procedure; because, we have fully coupled motions between the principal directions of the motions. To overcome this problem, we used a two-dimensional polynomial model to approximate the finite element displacement field. A linear solid model is used based on Sanders' shell theory. The first order piston theory employed to model the aerodynamic forces induced by the supersonic flow. Parametric studies for different thicknesses and aspect ratios carried-out in order to see how dynamic instability point is affected. Moreover, the effect of boundary condition on natural frequencies is also investigated.

CHAPTER 2 ARTICLE 1 - FINITE ELEMENT MODEL TO INVESTIGATE THE DYNAMIC INSTABILITY OF A RECTANGULAR PLATE SUBJECTED TO SUPERSONIC AIRFLOW

AOUNI A. LAKIS[1], HOSSEIN BAHRAMI-TORABI, YOUCEF KERBOUA

THIS CHAPTER WAS SUBMITTED TO THE JOURNAL OF FLUIDS AND STRUCTURES, AND THE MANUSCRIPT WAS ACCEPTED WITH MINOR REVISION AND MODIFICATION.

Mechanical Engineering Department, Polytechnique de Montréal, C.P. 6079, Succ. Centre-ville, Montréal, Québec, H3C 3A7, Canada

[1]CORRESPONDING AUTHOR

E-mail address: aouni.lakis@polymtl.ca (A.A.Lakis)
Fax: +1 514 340 4176.
Phone: +1 514 340 4711/4906

Abstract

In this paper, a numerical method is presented to study the dynamic behaviour of an isotropic rectangular plate subjected to aerodynamic loads induced by parallel supersonic airflow. A finite element model, based on bi-dimensional polynomial displacement functions and linear Piston theory, is used to study the dynamic behaviour of the solid plate coupled with aerodynamic loads. The developed approach is able to model flat plates and shallow shells in which the fluid-structure coupling at the interface is applied synchronously using a monolithic method. The solid model is based on Sanders' shell theory. The stiffness and damping matrices that result from application of the aerodynamic load are coupled with those obtained from a structural model and are calculated using analytical integration. By assembling the matrices, the global mass, damping and stiffness matrices for the plate are obtained and then dynamic equations of the governing problem are derived. The eigenvalues of the system are calculated using the reduction technique. The critical non-dimensional aerodynamic pressure of the airflow that induces flutter of the structure is determined for various boundary conditions and geometries. The obtained results are compared with other published research works and very good agreement is observed.

Keywords: Finite element, fluid-structure interaction, aerodynamic pressure, piston theory, frequency, flutter.

2.1 Introduction

Plates are widely used in structures commonly found in the aerospace, aeronautical, shipbuilding, and nuclear industries. All of these industrial fields are of major economic importance and require high safety levels. To avoid failures, it is therefore critical to have a good understanding of the dynamic behaviour of these structures when subjected to external loads. A large effort has been devoted by researchers to resolve many issues in this field, and a multitude of theoretical [1-15] and experimental works [16-21] have been completed during the past few decades. In 1992, Bismark [26] investigated linear structural models and underlined that due to hypersonic flight, new mathematical models must be included for accurate prediction of aerodynamic loads and for analysis of the aeroelastic stability of plates and shells. He also mentioned that, although the finite element method (FEM) provides a robust approach for analyzing complex geometries and various loading, it is still not fully utilized for many cases and there are limited results available to compare with other methods such as Rayleigh–Ritz and Galerkin.

Abbas et al. [33] used continuum mechanics as a basis to develop structural model by applying an absolute nodal coordinate formulation (ANCF) procedure. They considered both shear and transversal strains in their formulations. Linear piston theory was used to predict the aerodynamic load. In fact, this was the first time that ANCF was used for analyzing an isotropic plate element with different boundary conditions subjected to supersonic flow. They showed that the results obtained using ANCF have good agreement compared to the results in literature. Bloomhardt and Dowell [34] worked on noise reduction of transport aircraft in a subsonic regime. They used a plate model with linear potential flow theory to analyze the aeroelastic behavior of the wing. They considered two different boundary conditions. First, they considered all edges simply-supported and second, they considered three edges simply-supported and one edge (trailing edge) free. They concluded that for a specific boundary conditions, flutter dynamic pressure increases as the aspect ratio of the wing is increased. Moreover, flutter dynamic pressure for the case of the free trailing edge is higher than the case of all edges simply-supported for a fixed aspect ratio. Xie et al. [35] studied nonlinear flutter in supersonic flow for a cantilevered plate using the

Proper Orthogonal Decomposition (POD) method. They utilized Von Karman plate theory and first order piston theory in their analysis. They concluded that good convergence can be obtained if the number of POD modes are lower than the number of Rayleigh–Ritz modes and it also reduces computational effort. Gibbs and Dowell [38] studied the stability of rectangular plates in subsonic flow and validated their results with an experimental setup. They considered a linear structural model with an unsteady aerodynamic model to estimate the aerodynamic loads. They used Rayleigh-Ritz method to solve their numerical problems. To resemble a real wing structure, they considered different boundary conditions for their analysis. They validated their results for a combination of clamped and free boundary conditions to resemble a real wing structure. For each type of boundary conditions, they could see either flutter or divergence in their analysis. Kerboua et al. [30] investigated linear vibration analysis of a rectangular plate in water. They developed equations of motion using the finite element method and Sanders' shell theory. Polynomial and exponential functions were used to model the in-plane and out-of-plane displacement components. Moreover, they used velocity potential and Bernoulli's equation to determine the fluid load acting on the structure. They compared their results with both experimental and other analytical studies and a good agreement was found. Katsikadelis and Babouskos [31] studied flutter response of an isotropic thin plate in supersonic flow considering internal and external damping. Governing equations were derived from classical plate theory and first order piston theory. An Analog Equation Method (AEM) was employed to decouple the foregoing equations into one bi-harmonic as well as two Poisson's equations under fictitious excitation. These equations were solved by employing the boundary element method (BEM). Song and Li [36] investigated the effects of various boundary conditions and the accuracy of the assumed mode method (AMM) on the flutter characteristics of an isotropic rectangular plate subjected to supersonic flow. They employed classical thin plate theory to model structural motion along with piston theory to estimate aerodynamic loads. Equations of motion, derived by Hamilton's principle, were solved using the finite element method and AMM. They found that AMM is not as accurate as the finite element method and concluded that stiffer boundary conditions would substantially improve stability of the plate. Moreover, when the boundary of the structure is elastically restrained, mode veering will occur. Based on the Ye and Dowell model [25], Xie et al. [37] extended this work and studied a chaos phenomenon for a cantilevered plate in

supersonic flow. They showed that, with decreasing length-to-width ratio the critical dynamic pressure decreases. They employed time histories, phase trajectories, bifurcation diagrams, Poincaré plots and frequency spectra to identify the evolution of chaos. Xie and Xu [39] focused on semi-analytical proper orthogonal decomposition methods (S-POD and P-POD methods) and compared their results with Rayleigh–Ritz and Galerkin methods. They studied both cantilevered and simply-supported plates in supersonic flow. They found that the P-POD method is more efficient and accurate than the Galerkin method. Therefore, they recommended using P-POD and S-POD methods for the simply-supported and cantilevered plate, respectively. Mahran et al. [40] studied a linear isotropic trapezoidal plate wing and explored flutter and divergence using an F.E. approach. They used a linear vortex lattice method to carry out a divergence analysis and linear doublet lattice method for flutter analysis. Static condensation was employed to reduce in-plane degrees of freedom at each node and hence to reduce the computational burden. They concluded that, by increasing wing taper, divergence and flutter speeds of the plate increased. Ganji and Dowell [41] studied panel flutter in two-dimensional flow using the Enhanced Piston Theory (EPT). According to their conclusions, if the Mach number lies within a specific range ($1<M<\sqrt{2}$), flutter boundary and post-flutter response cannot be determined using full potential flow theory because this model calculates negative damping and predicts that the aeroelastic system is always unstable. By including higher order terms of reduced frequency in the solution, the model can accurately predict flutter and post flutter response [42]. They also noted that for $M>\sqrt{2}$, results obtained with lower order piston theory approach those calculated using Enhanced Piston Theory. Tian et al. [44] considered a trapezoidal wing in hypersonic flow and obtained governing equations using coupled von Karman's large deflection plate theory and third order piston theory. They subsequently integrated equations using the Rayleigh-Ritz method along with affine transformation and found that the flutter boundary is substantially influenced by increasing sweep angle at different cord-to-span ratios. Aravinth et al. [45] studied a trapezoidal wing subjected to parallel flow with different Mach numbers from subsonic to supersonic regimes. They used Enhanced Piston Theory [42] along with von Karman's large deflection plate theory to develop governing equations. A Jacobian transformation with a Rayleigh-Ritz approach was used to convert the cantilevered trapezoidal plate into a cantilevered square plate in order to solve nonlinear oscillations of a fluttering plate. They concluded that the amplitude of the limit cycle

increases with increasing the dynamic pressure. Moreover, by using EPT fewer modes are necessary to obtain a converged solution and as a consequence computational time is decreased. Lin et al. [46] investigated the flutter response of an elastic rectangular functionally-graded (FG) plate reinforced with carbon nanotubes in hypersonic airflow under an aero-thermal load. They considered coupled thermo-elastic effects by solving von-Karman plate theory in conjunction with Fourier's heat conduction equation along with third-order piston theory. They used finite difference and Galerkin methods to solve thermal and aeroelastic equations, respectively. In general, coupled and uncoupled approaches showed relative agreement in buckling, limit cycle oscillation (LCO) and chaos response but not in motion amplitudes and flutter response. Lakis et al. [24, 27] analyzed axisymmetric structures. They proposed displacement fields which exactly satisfied equilibrium equations. The dynamic model of cylindrical shells allows separation of variables in longitudinal and circumferential directions (in a cylindrical coordinate system), which makes obtaining an exact solution possible. This approach yields an accurate model and facilitates coupling of fluid-structure equations. However, in rectangular plates, obtaining exact solutions for equilibrium equations is not possible because the separation of variables remains impossible due to a fully coupled motion field at the principal directions of the motions (in a cartesian coordinate system). In this paper, to overcome this problem, a two-dimensional polynomial model is used to approximate the finite element displacement field. Linear solid model is developed based on Sanders' shell theory. First order piston theory models the aerodynamic forces induced by supersonic flow. Parametric studies for different thicknesses and aspect ratios are carried-out in order to see how the dynamic instability point is affected. The effect of boundary conditions on natural frequencies is also investigated. The originality of this work lies in the fact that a monolithic solid-fluid finite element model developed which is capable of simulating plates with any geometry (e.g., rectangular, circular). In addition, any boundary conditions can be applied at edges or in the middle of the plate. Also, the thickness and mechanical properties of the plate can vary at each point with/without structural discontinuities (i.e., holes).

2.2 Structural Model

In the present study, a flat finite element with four nodes (*i, j, k* and *l*) and six degrees of freedom at each node is used to obtain a solid structural model, see Figure (2). The kinematic equations are developed using Sanders' thin shell theory based on Love's first order approximation [23]. Membrane and bending effects are considered in this theory.

2.2.1 Kinematic Equations:

The displacement field of the middle surface of a flat plate may be expressed as a function of the in-plane displacements U and V in X and Y directions, respectively, and the transverse displacement W in the Z direction, according to the following equations:

$$U(x,y,t) = C_1 + C_2\frac{x}{A} + C_3\frac{y}{B} + C_4\frac{xy}{AB} \qquad (1)$$

$$V(x,y,t) = C_5 + C_6\frac{x}{A} + C_7\frac{y}{B} + C_8\frac{xy}{AB} \qquad (2)$$

$$W(x,y,t) = C_9 + C_{10}\frac{x}{A} + C_{11}\frac{y}{B} + C_{12}\frac{x^2}{2A^2} + C_{13}\frac{xy}{AB} + C_{14}\frac{y^2}{2B^2} + C_{15}\frac{x^3}{6A^3} + C_{16}\frac{x^2y}{2A^2B} + C_{17}\frac{y^2x}{2AB^2} + C_{18}\frac{y^3}{6B^3} + C_{19}\frac{x^3y}{6A^3B} + C_{20}\frac{x^2y^2}{4A^2B^2} + C_{21}\frac{xy^3}{6AB^3} + C_{22}\frac{x^3y^2}{12A^3B^2} + C_{23}\frac{x^2y^3}{12A^2B^3} + C_{24}\frac{x^3y^3}{36A^3B^3} \qquad (3)$$

Where: A and B are plate dimensions and C_j are unknown constants.

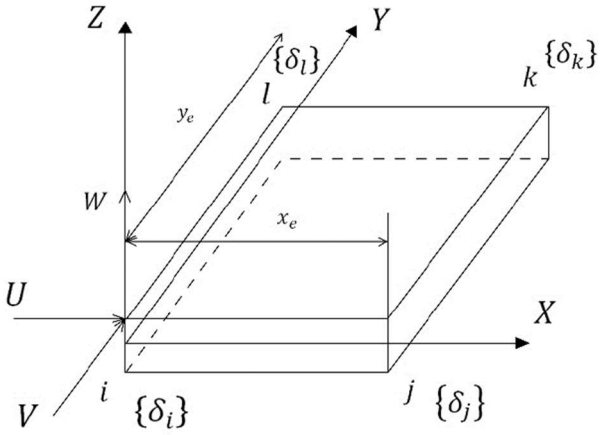

Figure 2: Geometry and displacement field of a typical element

In matrix form U, V and W can be written as follows:

$$\begin{Bmatrix} U \\ V \\ W \end{Bmatrix} = [R]\{C\} \qquad (4)$$

In the above equation, $[R]$ is a 3×24 matrix and $\{C\}$ is the unknown constant vector of order 24. Matrix R is presented in Appendix B.

Each element consists of four nodes and each node has six degrees of freedom. Therefore, displacement and nodal displacement vectors are, respectively given by Equations (5) and (6) as follows:

$$\{\delta\} = \left\{\{\delta_i\}^T, \{\delta_j\}^T, \{\delta_k\}^T, \{\delta_l\}^T\right\}^T \qquad (5)$$

$$\{\delta_i\} = \left\{U_i, V_i, W_i, \frac{\partial W_i}{\partial x}, \frac{\partial W_i}{\partial y}, \frac{\partial^2 W_i}{\partial x \partial y}\right\}^T \qquad (6)$$

By substituting Equations (1-3) into Equation (5), one can obtain:

$$\{\delta\} = [A]\{C\} \qquad (7)$$

Multiplying each side of Equation (7) by $[A]^{-1}$, the following expression can be found for vector $\{C\}$.

$$\{C\} = [A]^{-1}\{\delta\} \qquad (8)$$

$[A]^{-1}$ terms are found in Appendix B. Using Equations (8) and (4), the displacement field can be written as follows:

$$\begin{Bmatrix} U \\ V \\ W \end{Bmatrix} = [R][A]^{-1}\{\delta\} = [N]\{\delta\} \qquad (9)$$

In the above equation, matrix $[N]$ is the displacement shape functions of order 3×24.

2.2.2 Strain displacement relations

According to Sanders theory [23], strains for a rectangular plate are related to displacement through the following equation:

$$\begin{Bmatrix} \varepsilon_{xx} \\ \varepsilon_{yy} \\ 2\varepsilon_{xy} \\ k_x \\ k_y \\ k_{xy} \end{Bmatrix} = \begin{Bmatrix} \frac{\partial U}{\partial x} \\ \frac{\partial V}{\partial y} \\ \frac{\partial V}{\partial x} + \frac{\partial U}{\partial y} \\ \frac{-\partial^2 W}{\partial x^2} \\ \frac{-\partial^2 W}{\partial y^2} \\ \frac{-2\partial^2 W}{\partial x \partial y} \end{Bmatrix} \qquad (10)$$

Sander's theory in comparison to Love's first approximation has the following advantages:

1. It is more realistic because all strains vanish for small rigid-body motions of the shell whereas for Love's theory they do not.

2. In Sanders' theory, the number of stress unknowns are reduced from 10 to 8 by using a symmetric approximation in the expressions of the resultants in terms of integrals of stress through the thickness of the shell.

3. The expressions for the stress quantities satisfy the equations of equilibrium identically [23].

By introducing the displacements given in Equation (9) into the above strain-displacement relationship, one obtains the strain vector as a function of nodal displacements for each finite element.

$$\{\varepsilon\} = [\mathrm{Q}][A]^{-1}\{\delta\} = [B]\{\delta\} \qquad (11)$$

Where: Q matrix is order of (6×24) and is given in Appendix B.

2.2.3 Constitutive equations:

To obtain structural matrices, the relationship between stresses and strains must be defined. For an isotropic rectangular plate, Equation (12) is written to relate the strain field to the stress field.

$$\{\sigma\} = [P]\{\varepsilon\} \qquad (12)$$

Where $[P]$ is the elasticity matrix coefficients of order (6×6) given Appendix A.

By substituting Equation (11) into Equation (12), the stress field can be rewritten as follows:

$$\{\sigma\} = [P][B]\{\delta\} \qquad (13)$$

Using the standard procedure of the finite element method, the mass $[m]^e$and stiffness $[k]^e$ matrices for each finite element can be expressed by Cook [28]:

$$[k]^e = \iint_A [B]^T[P][B]dA \qquad (14)$$

$$[m]^e = \rho_s h \iint_A [N]^T[N]dA \qquad (15)$$

Where h is the thickness of the plate and ρ_s is the material density. Mass $[m]^e$and stiffness $[k]^e$ matrices can be obtained by substituting $[B] = [\mathrm{Q}][A]^{-1}$ and $[N] = [R][A]^{-1}$into Equations (14) and (15):

$$[k]^e = [[A]^{-1}]^T(\int_0^{y_e}\int_0^{x_e}[Q]^T[P][Q]dxdy)[A]^{-1} \qquad (16)$$

$$[m]^e = \rho h[[A]^{-1}]^T(\int_0^{y_e}\int_0^{x_e}[R]^T[R][Q]dxdy)[A]^{-1} \qquad (17)$$

In the above equations, x_e and y_e are dimensions of an element in X and Y directions, respectively. These integrals are computed in MATLAB software.

2.3 Aeroelastic model

Elastic structures subjected to supersonic flow may lose their dynamic stability. When a plate in supersonic flow is considered, there is an aerodynamic load exerted on the plate due to the effect of flow on the structure. This load changes the global matrices of the structure by adding virtual damping and stiffness induced by flow to the dynamic equations.

The general equation governing fluid structure interaction in the case of an elastic flat plate subjected to parallel supersonic flow is as follows:

$$[M_s]\{\ddot{\delta}_G\} + \left[C_f\right]\{\dot{\delta}_G\} + \left[[K_s] - \left[K_f\right]\right]\{\delta_G\} = \{0\} \qquad (18)$$

In Equation (18), the terms s and f are the structural and fluid effects, respectively. δ_G is the global displacement vector of the plate. In the above equation, structural damping is not considered, because it is dependent on the thickness of the membrane and for thin shells it is negligible in comparison to the aerodynamics and inertial forces.

Piston theory was introduced into aeroelasticity in a linearized form by Ashley and Zartarian [22]. It is an efficient tool that provides an approximation for the aerodynamic pressure applied on an elastic structure with remarkable accuracy whenever the Mach number is approximately between 2.5 to 4.5 [22].

To model the effects of supersonic flow on an elastic plate, we calculate the aerodynamic pressure and then integrate it over the solid-fluid interface of each finite element. The pressure equation for piston theory which is applicable to supersonic flow with Mach number over 1.7 (M > 1.7), is used in this paper and expressed as follows [43]:

$$P = \frac{-2Q_\infty}{\sqrt{M_\infty^2 - 1}}\left[\frac{\partial W}{\partial x} + \frac{1}{V_\infty}\left(\frac{M_\infty^2 - 2}{M_\infty^2 - 1}\right)\frac{\partial W}{\partial t}\right] \quad (19)$$

In the above equation, W, Q_∞, M_∞ and V_∞ are displacement vector, dynamic pressure, Mach number and free stream velocity respectively. The correction factor for curvature has been omitted as it has been proven in previous works that it doesn't have a significant effect [32]. Moreover, W can be rewritten based on shape functions using Equation (9).

The fluid-induced force vector can be written for each finite element in terms of equivalent nodal forces as follows:

$$\{F_a\}^e = \int_A [N]^T \{P_a\}\, dA = \int_A [[A]^{-1}]^T [R]^T \begin{Bmatrix} 0 \\ 0 \\ P \end{Bmatrix} dA \quad (20)$$

$[N]$ is the displacement shape function matrix. $\{P_a\}$ is the aerodynamic pressure which may be rewritten as function of nodal displacements based on Equation (19) as follows:

$$\{P_a\} = \frac{-2Q_\infty}{\sqrt{M_\infty^2 - 1}}\left[[R']^T [[A]^{-1}]^T \{\delta\} + \frac{1}{V_\infty}\left(\frac{M_\infty^2 - 2}{M_\infty^2 - 1}\right)[R]^T [[A]^{-1}]^T \{\dot{\delta}\}\right] \quad (21)$$

The latter equation is obtained by introducing the displacement functions of Equation (9) into Equation (19). $[R']$ is a matrix of order (3×24) obtained by working out derivatives of $[R]$ with respect to x.

Substituting Equation (21) into Equation (20) one obtains the aerodynamic load vector as follows:

$$\{F_a\}^e = Z_1 \int_A [[A]^{-1}]^T [R]^T [[R']^T [[A]^{-1}]^T \{\delta\}] dA$$

$$+ Z_1 . Z_2 \int_A [[A]^{-1}]^T [R]^T \left[[R]^T [[A]^{-1}]^T \{\dot{\delta}\}\right] dA \quad (22)$$

Where:

$Z_1 = \frac{-2Q_\infty}{\sqrt{M_\infty^2 - 1}}$ and $Z_2 = \frac{1}{V_\infty}\left(\frac{M_\infty^2 - 2}{M_\infty^2 - 1}\right)$

Based on Equation (22), the aerodynamic stiffness and damping for one element will be obtained as follows:

$$[k_a] = Z_1 \int_{A_e} [[A]^{-1}]^T [R]^T [[R']^T [[A]^{-1}]^T] dxdy \quad (23)$$

$$[c_a] = Z_1 . Z_2 \int_A [[A]^{-1}]^T [R]^T [[R]^T [[A]^{-1}]^T] dxdy \quad (24)$$

Equations (23) and (24) are aerodynamic elementary matrices that must be added to solid equations.

2.4 Global matrices and eigenvalue problem

The rectangular plate is subdivided into small rectangular finite elements, each of which has its own structural and aerodynamic matrices computed in Equations (14-15) and Equations (23-24), respectively. The global matrices mentioned in dynamic Equation (18) governing the coupled fluid-structure system are determined by superimposing elementary matrices developed above and by taking the applied boundary conditions into account.

The eigenvalue problem of the governing dynamic Equation (18) may be solved by means of the equation-reduction technique. Equation (18) may be rewritten as follows:

$$\begin{bmatrix} [0] & [M_s] \\ [M_s] & [C_f] \end{bmatrix} \begin{Bmatrix} \{\ddot{\delta}_G\} \\ \{\dot{\delta}_G\} \end{Bmatrix} + \begin{bmatrix} -[M_s] & [0] \\ [0] & \left[[K_s] - [K_f]\right] \end{bmatrix} \begin{Bmatrix} \{\dot{\delta}_G\} \\ \{\delta_G\} \end{Bmatrix} = \{0\} \quad (25)$$

Without considering fluid effects, Equation (25) may be simplified to:

$$[M_s]\{\ddot{\delta}_G\} + [K_s]\{\delta_G\} = \{0\} \qquad (26)$$

Natural frequencies and mode shapes for such a system are obtained by solving the following equation:

$$Det\left[[K_s] - \omega^2[M_s]\right] = 0 \qquad (27)$$

This approach was used to validate free vibration analysis results.

When an elastic plate is subjected to supersonic flow, the natural frequencies and mode shapes of Equation (25) are calculated by solving the following equation:

$$|[D] - \Lambda[I]| = 0 \qquad (28)$$

Where, $[D] = \begin{bmatrix} [0] & [I] \\ \left[[K_s] - [K_f]\right]^{-1}[M_s] & \left[[K_s] - [K_f]\right]^{-1}[C_f] \end{bmatrix} = 0$

In the above equation, $[I]$ is the identity matrix and $\Lambda = -\frac{1}{i\omega^2}$ where ω is the natural frequency.

To obtain natural frequencies and mode shapes, two separate codes were developed in FORTRAN and MATLAB software. In FORTRAN, DEVLCG subroutine was used to determine natural frequencies and mode shapes. In MATLAB, natural frequencies and mode shapes were obtained by using POLYEIG command. Both results were in good agreement.

2.5 Results and discussion

In this section, the fluid-structure model developed above is used to calculate the dynamic behavior of plates subjected to supersonic flow. Several boundary conditions and geometrical configurations were studied to investigate the vulnerability of plates under aerodynamic loads. First, the requisite mesh size of convergence for the problem was obtained, see Figure (4). Then, the problem was studied based on obtained mesh size. The results were validated at each step.

The first set of calculations concerns a simply-supported (SSSS) rectangular plate as studied in reference [29]. For all cases studied in this paper, the boundary condition of each side of the rectangular plate is cited according to the order shown in Figure (3). In this paper, no aerodynamic loading is accounted for vibration analysis of the plate. Examples of boundary conditions are illustrated in Figure (5). The physical properties of the solid plate are: $E = 196\ GPa,\ \rho = 7860\ kg/m^3,\ h = 2.54\ mm,\ \nu = 0.3,\ A = 609.6\ mm$ and $B = 304.8\,mm$. The

computed natural frequencies are shown in both Table 1 and Figure (4) for various mesh sizes (n_x, n_y) along the x and y coordinates, respectively. It can be concluded that, for the first four fundamental modes, twenty-five finite elements (5×5) are sufficient to reach mesh independency, whereas for higher modes like mode 5 and 6 and more, considering at least 64 elements, is a good one to have more accurate results.

The aerodynamic pressure presented in Equation (21) was used to calculate the natural frequencies of a flat plate subjected to external supersonic flow. The objective was to validate our numerical model through comparison with the case studied in reference [36]. For this purpose, a plate with geometry and mechanical properties: E= 210 GPa, $\rho = 7930\ kg/m^3$, $h = 0.001m$ $\nu = 0.33$, $A = B = 0.1\ m$, is considered [36]. In Equation (21), Q_∞ is increased progressively from zero to higher values where for example, for fully simply supported plate (SSSS), this range is between 0 to 248×10^5. Then, frequency is calculated at each step. To enable comparison of the results with reference [36], a non-dimensional aerodynamic pressure $\lambda = 2Q_\infty A^3/\beta K$ is defined, where $\beta = \sqrt{{M_\infty}^2 - 1}$ and $K = Eh^3/12(1-\nu^2)$. Results obtained for plates with various boundary conditions (FSFS, CSCS and SSSS) are shown in Figures (6) to (8) for the first fundamental modes. Article [36] reports results for these plates using two different methods, the assumed mode method and the finite element method. The critical dynamic pressure obtained for a plate which is simply-supported (SSSS) on four sides shows very good agreement between the two methods. However, for the other boundary conditions (CSCS and FSFS), a significant difference was found. Our results agree perfectly with those of the finite element method in reference [36], using a very low number of finite elements (see Figures (6) to (8)). As we used only 25 elements for obtaining our results, current method is much faster than reference [36] where they used 225 elements for case SSSS and 441 elements for cases FSFS and CSCS to obtain good results. The critical pressures inducing dynamic instability of the "flutter" type for each case are cited in Table 2. Flutter occurred when two modes coincide at the same critical pressure (Figures (6) and (8)). A perfect agreement between our results and those of Song et al. [36] is seen.

The validations made above encouraged us to employ the developed model to study the effect of boundary conditions and geometrical ratios on the dynamic stability of plates in contact with

supersonic flow. The reference plate used to carried out these calculations is made of aluminium with the following physical properties: E = 69 GPa, ρ = 2750 kg⁄m^3, h = 1 mm, ν = 0.33, and A = B = 0.1 m. Table 3 and Table 4 give the critical non-dimensional aerodynamic pressure inducing flutter or divergence type instabilities (by increasing non-dimensional aerodynamic pressure, when natural frequency decreases and goes near 0, divergence type instabilities will be occurred). The results listed in Table 3 were calculated for various boundary conditions and geometrical ratios A/B. The dimension A was maintained constant while B was varied from 0.05 m to 0.4 m. Additionally, Table 4 gives the critical non-dimensional aerodynamic pressure inducing flutter or divergence type instabilities for various thicknesses where A = B = 0.1 m.

Figures were added for some of the cases analyzed to reveal how the dynamic behaviour of the plate progresses and to identify the modes in which flutter or divergence occur (see Figures (9) to (12)). It is evident that boundary conditions play a major role in the dynamical stability of the structure. More structural support is equivalent to an increased stability margin at higher supersonic flow velocities. However, by examining the obtained results, it is indicated that adding support to edges along the flow direction or in the direction perpendicular to the flow have different effects on the dynamic stability quantitatively and qualitatively. For example; Cases 2 and 3 in Table 3 have a geometrical ratio A/B=0.5. The unique difference between these two cases is the flow direction with respect to the clamped sides (i.e., CFCF versus FCFC). For the same fluid-structure interaction area, the plate in Case 2 undergoes a flutter type instability at λ = 207.88. For Case 3 on the other hand, a divergence type instability occurs at a much lower dimensionless dynamic pressure; λ = 19.75 (see Figure (9)). At constant thickness, if the plate does not have any supported edges parallel to the flow direction, aspect ratio variation does not significantly affect stability results (see Cases 2, 4 and 6 in Table 3). Moreover, by increasing the aspect ratio (A/B), the critical pressure increased in all boundary conditions except for case 4 (see Table 3). Most boundary conditions showed either pure divergence or flutter instability, but CFCF initially experienced divergence-type instability (A/B≤1), and by increasing the aspect ratio, flutter became the dominant instability (Table 3). In general, removing boundary condition of the outer edge (side 2 in Figure (3)) made the plate more prone to divergence instability (Tables 3 and 4). In all boundary conditions, increasing the plate thickness increased critical dynamic pressure (λ_{cr}) because of improving structural stiffness (Table 4) but did not alter the

instability type (flutter or divergence) since the plate aspect ratio (for example Case 3 in Table 3) and boundary conditions determine the instability type.

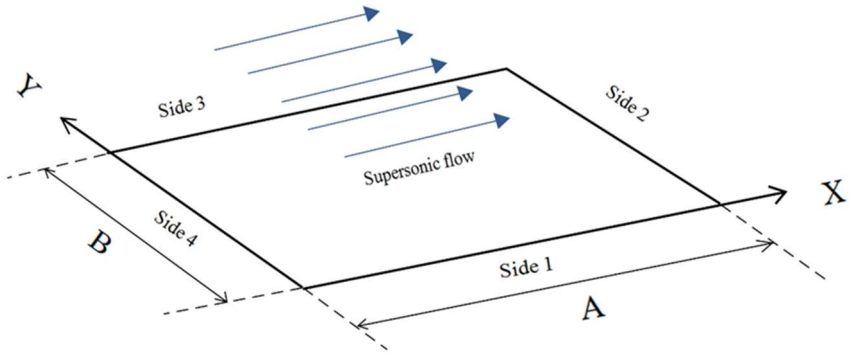

Figure 3: Flow direction and order of boundary conditions, CFCF is a clamped-free-clamped-free plate, respectively, at sides 1, 2 3 and 4

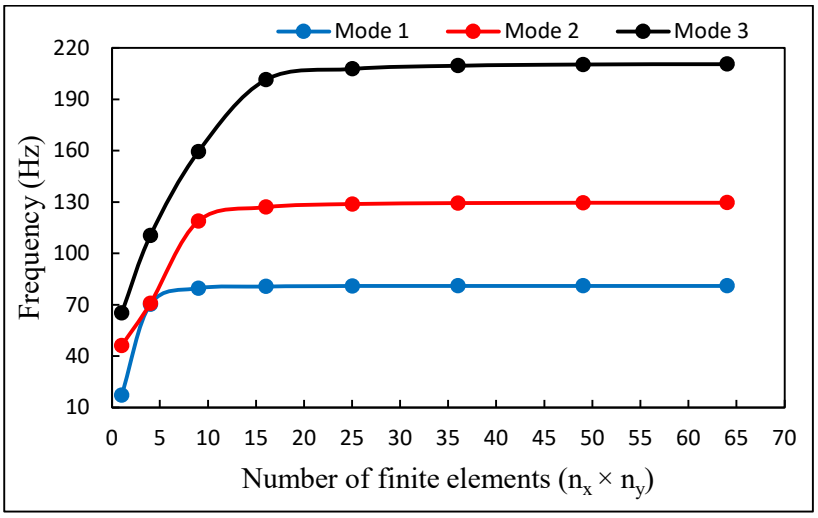

Figure 4: Mesh convergence as a function of the number of quadrilateral finite elements of a simply- supported (SSSS) rectangular plate

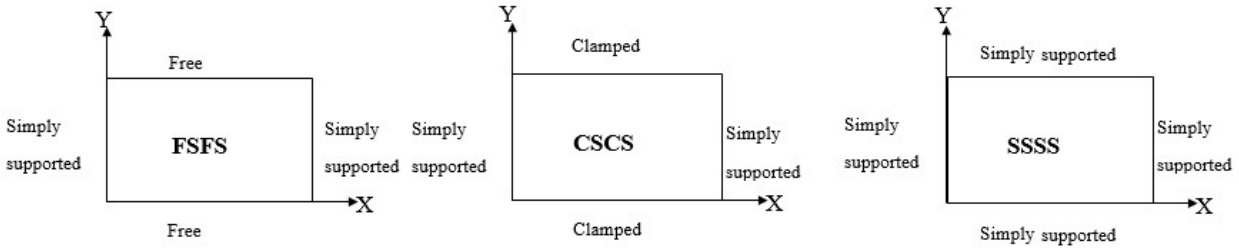

Figure 5: Some examples of boundary conditions designation (FSFS, CSCS and SSSS)

Table 1: Natural frequency (Hz) of a simply-supported (SSSS) rectangular plate compared to analytical and numerical solutions

	Present	Reference [29]	ANSYS (Shell 63)
Mode 1	81.00	82.93	80.99
Mode 2	128.86	133.44	129.33
Mode 3	207.84	213.72	209.86

Table 2: Critical non-dimensional aerodynamic pressure (λ_cr) inducing flutter for various boundary conditions

Boundary conditions	Critical non-dimensional aerodynamic pressure λ_{cr}			Flutter mode number
	Present FEM	FEM of Ref. [36]	AMM of Ref. [36]	
SSSS	511.38	512	512	1 and 2
FSFS	332.60	336	287	2 and 3
CSCS	548.80	546	428	1 and 2

Table 3: Critical non-dimensional aerodynamic pressure (λ_cr) inducing flutter (or divergence*) as a function of geometrical ratios A/B

Geometrical ratio A/B	Case 1 (SSSS)	Case 2 (FCFC)	Case 3 (CFCF)	Case 4 (FFFC)	Case 5 (CFFF)	Case 6 (FCFF)	Case 7 (SFSS)
0.25	-	-	3.58*	2.06*	1.40	10.40	3.7*

0.50	128.88	207.88	19.75*	2.04*	5.40	27.02	3.71*
0.75	145.51	205.80	64.03*	2.02*	10.39	38.45	13.3*
1.00	168.38	205.80	155.08*	2.00*	17.46	41.57	38.35*
1.25	203.72	205.80	216.20	1.99*	27.02	42.61	85.23*
1.50	245.30	203.72	268.17	1.97*	39.91	42.61	148.63*
1.75	299.35	203.72	336.77	1.96*	58.21	41.57	234.9*
2.00	361.71	201.64	422.00	1.95*	85.65	41.57	351.32*

Table 4: Critical non-dimensional aerodynamic pressure (λ_cr) inducing flutter (or divergence*) for various thickness ratios (href=1 mm and A=B=0.1 m).

Thickness ratio h/h_{ref}	(SSSS)	(FCFC)	(CFCF)	(FFFC)	(CFFF)	(FCFF)	(SFSS)
0.25	2.70	3.20	2.42*	0.03*	0.27	0.67	0.60*
0.50	21.83	25.57	19.33*	0.25*	2.16	5.20	4.78*
0.75	69.64	86.48	65.48*	0.84*	7.38	17.67	16.11*
1.0	168.38	205.80	155.08*	2.00*	17.46	41.58	38.35*
1.25	328.45	399.13	301.43*	3.91*	34.09	82.11	75.04*
1.50	571.67	690.16	523.86*	6.74*	58.62	141.36	129.30*
1.75	904.28	1093.45	832.35*	10.69*	92.51	224.51	205.80*
2	1340.80	1633.94	1241.04*	16.01*	138.24	332.60	307.25*

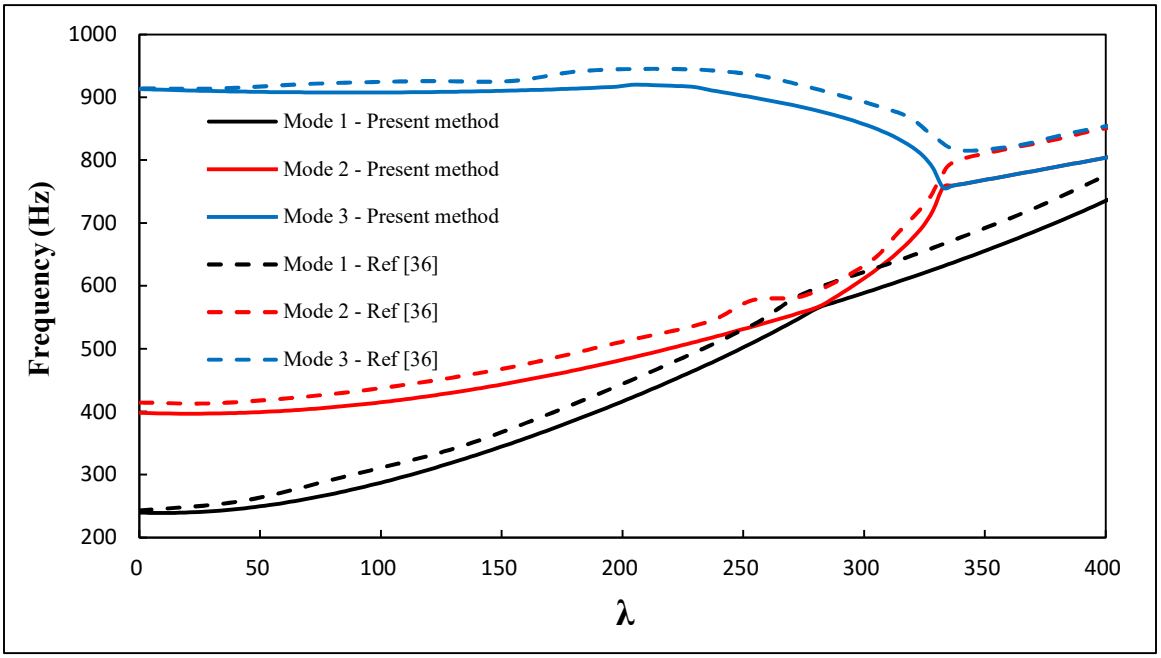

Figure 6: Natural frequency variation as a function of the non-dimensional aerodynamic pressure for a FSFS plate

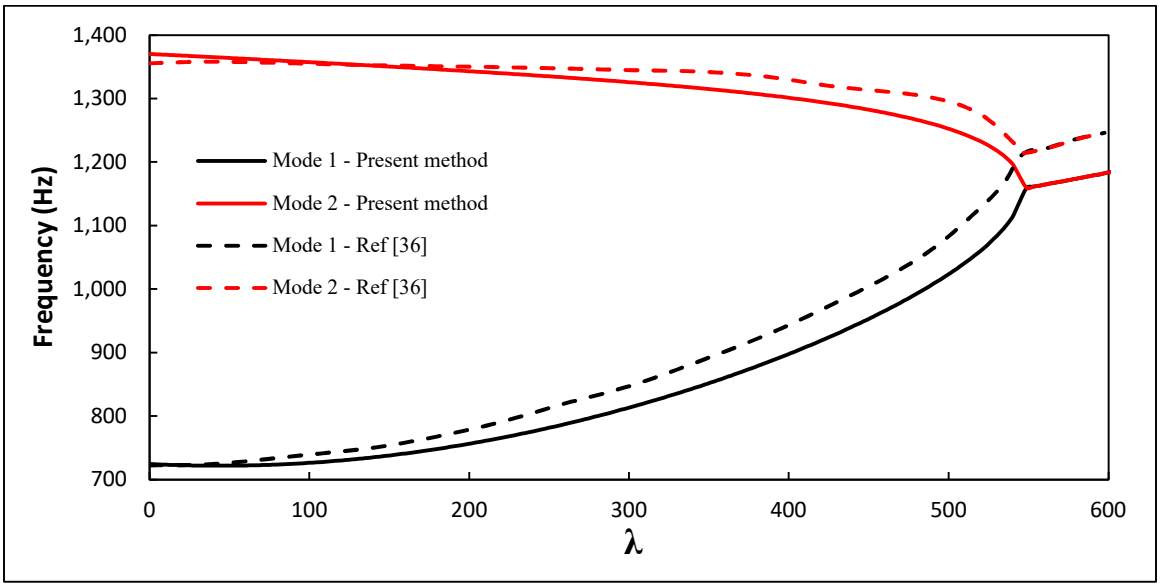

Figure 7: Natural frequency variation as a function of the non-dimensional aerodynamic pressure for a CSCS plate

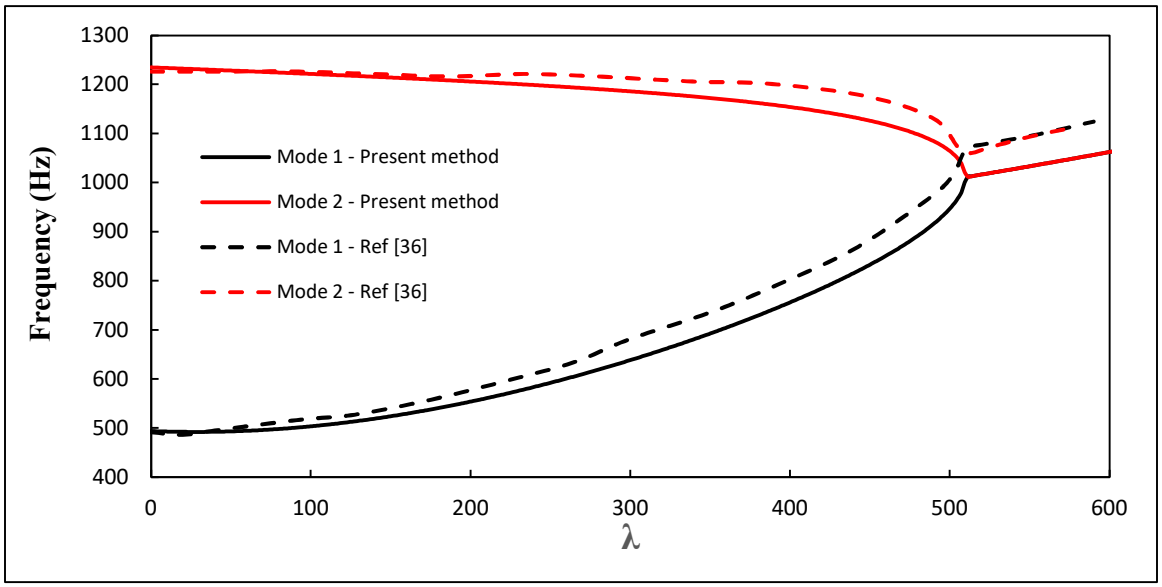

Figure 8: Natural frequency variation as a function of the non-dimensional aerodynamic pressure for a SSSS plate

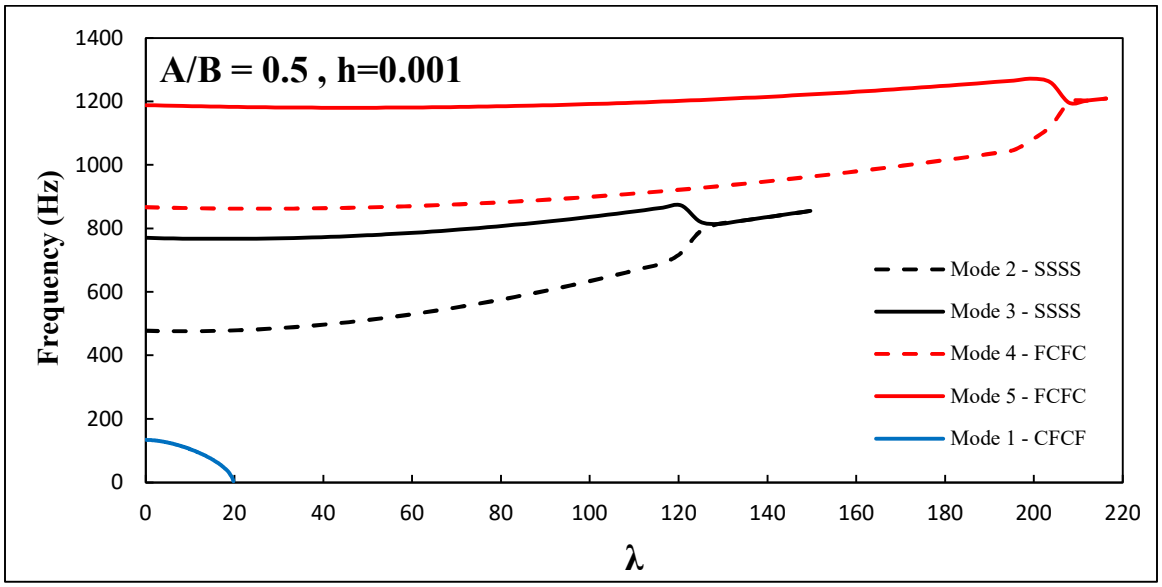

Figure 9: Natural frequency variation as a function of the non-dimensional aerodynamic pressure for an Aluminium plate

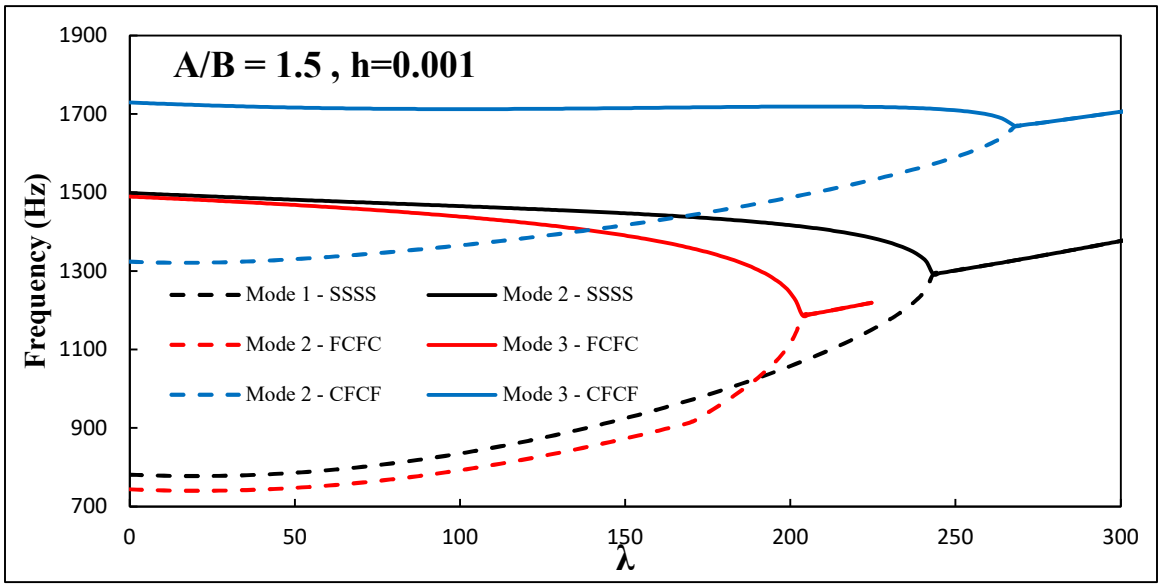

Figure 10: Natural frequency variation as a function of the non-dimensional aerodynamic pressure for an Aluminium plate

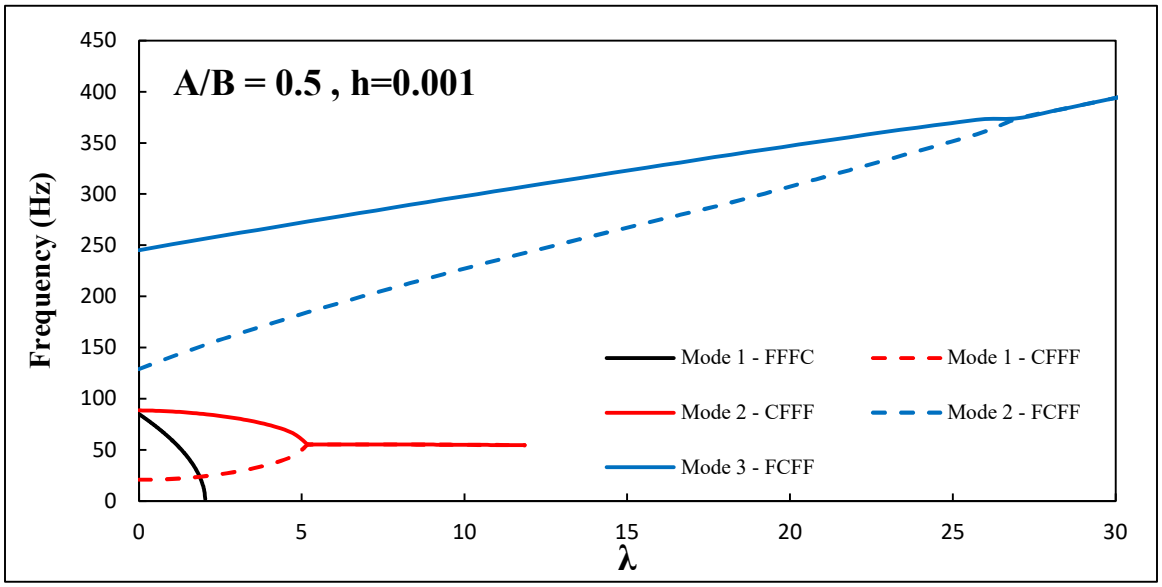

Figure 11: Natural frequency variation as a function of the non-dimensional aerodynamic pressure for an Aluminium plate

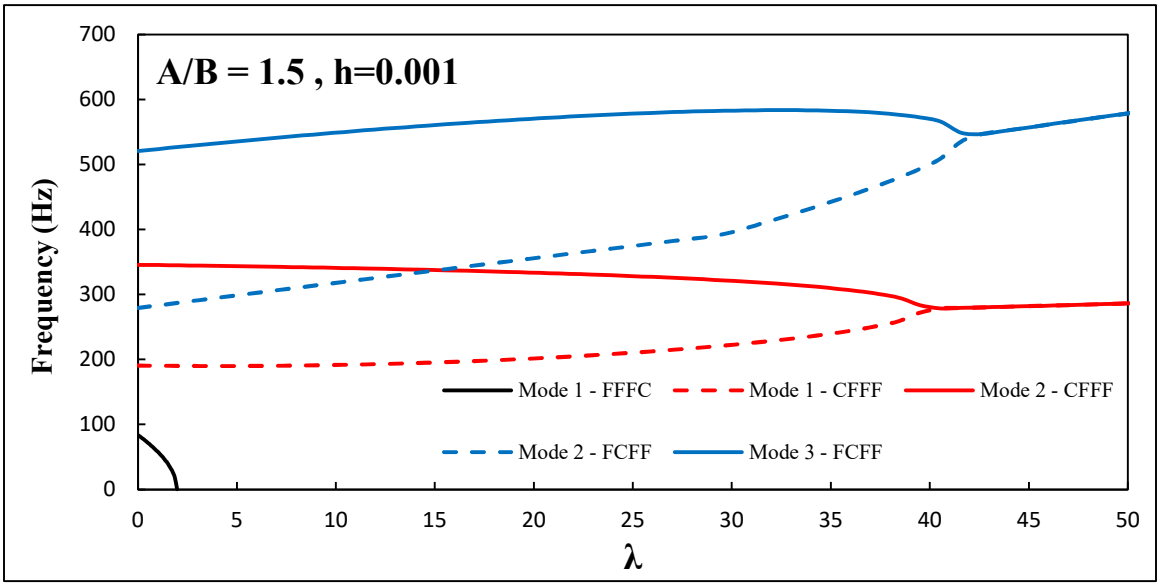

Figure 12: Natural frequency variation as a function of the non-dimensional aerodynamic pressure for an Aluminium plate

2.6 Conclusion

A new fluid-structure finite element model is presented to study the dynamic stability of rectangular plates subjected to parallel supersonic flow. The solid model uses linear Sanders' shell theory. The quadrilateral finite element shape functions are two-dimensional polynomial functions of order three for the transverse displacement and of order two for the in-plane displacements. The solid model are coupled with the first-order piston theory to model the aerodynamic pressure field. Calculations were performed for plates with various geometrical properties and boundary conditions. Two kinds of dynamic instability were observed in our results: the coupled-mode flutter and the divergence type instability. Cantilevered plates may lose their stability first through divergence and then by flutter due to coupling of the modes. The results obtained using the present model were validated against the existing works in literature and excellent agreement was found. This approach makes it possible to model plates with mechanical properties varying from one point to another in the structure or having geometric discontinuities. The developed method has the flexibility to model non-homogenous materials and discontinued structures.

2.7 References

[1] Vlasov VZ (1951), Basic differential equations in the general theory of elastic shells, NACA TM 1241.

[2] Stroud WJ (1963), Elastic constants for bending and twisting of corrugation-stIffened panels, NASA TR-R-166.

[3] Dowell EH (1966) Nonlinear oscillations of a fluttering plate I. AIAA J 4(7):1267–1275

[4] Dowell EH (1967) Nonlinear oscillations of a fluttering plate II. AIAA J 5(10):1856–1862

[5] Olson MD (1967), Finite elements applied to panel flutter, AIAA J 5, 2267-2270.

[6] Librescu L and Malaiu E (1968), Supersonic flutter of circular cylindrical heterogeneous orthotropic thin panels of finite length, J Sound Vib 8(3), 494-512.

[7] Dixon SC and Hudson ML (1969), Flutter boundary for simply supported unstiffened cylinders, AIAA J, 7(7), 1390-1391.

[8] Olson MD (1970), Some flutter solutions using finite elements, AIAA J 8, 747-752.

[9] Erickson LL, Supersonic flutter of sandwich panels; effect of face bending stiffness, rotary inertia, and orthotropic core shear stiffnesses (1971), NASA TND-6427.

[10] Leissa AW (1973), Vibration of shells, NASA SP-288.

[11] Bismarck-Nasr MN (1977), Finite element method applied to the flutter of two parallel elastically coupled flat plates, Int J Num Meth Engng 11, 1188-1193.

[12] Singa Rao K and Venkateswara Rao G (1983), Nonlinear supersonic flutter of panels considering shear deformation and rotary inertia, Int J Compt and Str'll.et 17(3), 361-364.

[13] Chen WH and Lin HC (1985), Flutter analysis of thin cracked panels using the finite element method, AIAA J. 23(5), 795-801.

[14] Sarma BS and Varadan TK (1988), Nonlinear panel flutter by finite-element method, AIAA .126(5), 566-574.

[15] Lin KJ, Lu PJ, and Tarn JQ (1989), Flutter analysis of composite panels using high-precision finite elements, Int J Compt and Struct 33(2), 561-574.

[16] Lock, M. H. and Fung, Y. C., "Comparative Experimental and Theoretical Studies of the Flutter of Flat Panels in a Low Supersonic Flow," AFOSR TN 670, May 1961, Guggenheim Aeronautical Lab., California Institute of Technology, Pasadena, Calif.

[17] Hess, R. W. and Gibson, F. W., "Experimental Investigation of the Effects of Compressive Stress on the Flutter of a Curved Panel and a Flat Panel at Supersonic Mach Numbers," TN D-1386, Oct. 1962, NASA.

[18] Dowell, E. H. and Voss, H. M., "Experimental and Theoretical Panel Flutter Studies in the Mach Number Range 1.0 to 5.0," TDR 63-449, Dec. 1963, Aeronautical Systems Division,. United States Air Force; also AIAA Journal, Vol. 3, No. 12, Dec. 1965, pp. 2292 2304.

[19] Shideler, J. L., Dixon, S. C., and Shore, C. P., "Flutter at Mach 3 Thermally Stressed Panels and Comparison with Theory for Panels with Edge Rotational Restraint," TN D-3498, Aug. 1966, NASA.

[20] Muhlstein, L., Jr., Gaspers, P. A., Jr., and Riddle, D. W., "An Experimental Study of the Influence of the Turbulent Boundary Layer on Panel Flutter," TN D-4486, 1968, NASA.

[21] Dowell, E. H., "Theoretical-Experimental Correlation of Plate Flutter Boundaries at Low Supersonic Speeds," AIAA Journal, Vol. 6, No. 9, Sept. 1969, pp. 1810-1811.

[22] Holt Ashley, Garabed Zartarian, "Piston Theory-A New Aerodynamic Tool for the Aeroelastician", Presented at the Aeroelasticity Session, Twenty-Fourth Annual Meeting, IAS, New York, January 23-26, 1956.

[23] Sanders Jr, J.L., An improved first-approximation theory for thin shells. NASA Rep., 1959.

[24] AA Lakis, MP Paidoussis, "Dynamic analysis of axially non-uniform thin cylindrical shells", Journal of Mechanical Engineering Science, vol 14, Feb. 1972, pp. 49-71.

[25] Dowell, E. and W. Ye, Limit cycle oscillation of a fluttering cantilever plate. AIAA journal, 1991. 29(11): p. 1929-1936.

[26] Bismarck-Nasr MN, "Finite element analysis of aeroelasticity of plates and shells," Appl Mech Rev vol 45, no 12, part 1, December 1992

[27] A Selmane, AA Lakis, "Non-linear dynamic analysis of orthotropic open cylindrical shells subjected to a flowing fluid", Journal of Sound and Vibration, vol 202, April 1997, pp. 67-93.

[28] D. Cook, D.S. Malkus, M.E. Plesha, R.J. Witt, Concepts and Applications of Finite Element Analysis, 4th edition, John, Wiley & Sons, Inc., 2002.

[29] Y Kerboua, Aouni A Lakis, Marc Thomas, L Marcouiller, "Hybrid method for vibration analysis of rectangular plates", Journal of Nuclear engineering and design, vol 237, April 2007, pp. 791-801.

[30] Kerboua, Y., et al., "Vibration analysis of rectangular plates coupled with fluid", Applied Mathematical Modelling, 2008. 32(12): p. 2570-2586.

[31] Katsikadelis, J. and N. Babouskos, "Nonlinear flutter instability of thin damped plates: A solution by the analog equation method", Journal of Mechanics of Materials and structures, 2009. 4(7): p. 1395-1414.

[32] Farhad Sabri, Aouni A Lakis, "Finite element method applied to supersonic flutter of circular cylindrical shells", AIAA journal, vol 48, January 2010, p. 73-81.

[33] Laith K. Abbas · Xiaoting Rui · P. Marzocca, "Panel flutter analysis of plate element based on the absolute nodal coordinate formulation", Journal of Multibody System Dynamics, July 2011, p. 135–152.

[34] Elizabeth M. Bloomhardt, Earl H. Dowell, "A Study of the Aeroelastic Behavior of Flat Plates and Membranes with Mixed Boundary Conditions in Axial Subsonic Flow", 52nd AIAA/ASME/ASCE/AHS/ASC Structures, Structural Dynamics and Materials Conference
 19th 4 - 7 April 2011, Denver, Colorado

[35] Dan Xie, Min Xu, Earl H.Dowell, "Projection-free proper orthogonal decomposition method for a cantilever plate in supersonic flow", Journal of Sound and Vibration, 333 (2014) p. 6190–6208.

[36] Song, Z.-G. and F.-M. Li, "Investigations on the flutter properties of supersonic panels with different boundary conditions. International Journal of Dynamics and Control", 2014. 2(3): p. 346-353.

[37] Xie, D., et al., "Observation and evolution of chaos for a cantilever plate in supersonic flow", Journal of Fluids and Structures, 2014. 50: p. 271-291.

[38] S. Chad Gibbs, Ivan Wang, Earl H. Dowell, "Stability of Rectangular Plates in Subsonic Flow with Various Boundary Conditions", Journal of Aircraft, Vol. 52, No. 2, March–April 2015.

[39] Xie, D. and M. Xu, "A comparison of numerical and semi-analytical proper orthogonal decomposition methods for a fluttering plate", Journal of Nonlinear Dynamics, 2015. 79(3): p. 1971-1989.

[40] Mahran, M., H. Negm, and A. El-Sabbagh, "Aero-elastic characteristics of tapered plate wings. Finite Elements in Analysis and Design", 2015. 94: p. 24-32.

[41] Ganji, H.F. and E.H. Dowell, "Panel flutter prediction in two dimensional flow with enhanced piston theory. Journal of Fluids and Structures", 2016. 63: p. 97-102.

[42] Dowell, E.H. and H.F. Ganji, "Investigation of higher order effects in linear piston theory", Mathematics in Engineering, Science & Aerospace (MESA), 2016. 7(1).

[43] Grover, N., B. Singh, and D. Maiti, An inverse trigonometric shear deformation theory for supersonic flutter characteristics of multilayered composite plates. Aerospace Science and Technology, 2016. 52: p. 41-51.

[44] Tian, W., et al., "Analysis of nonlinear aeroelastic characteristics of a trapezoidal wing in hypersonic flow", Journal of Nonlinear Dynamics, 2017. 89(2): p. 1205-1232.

[45] Aravinth, D., et al. "Dynamic Aeroelasticity of a Trapezoidal Wing Using Enhanced Piston Theory", 2018, AIAA/ASCE/AHS/ASC Structures, Structural Dynamics, and Materials Conference.

[46] Lin, H., et al., "Studies for aeroelastic characteristics and nonlinear response of FG-CNT reinforced composite panel considering the transient heat conduction", Journal of Composite Structures, 2018. 188: p. 470-482.

CHAPTER 3 GENERAL DISCUSSION

3.1 Motive

Plates are broadly used in different industries including aerospace, shipbuilding, and in the nuclear industry.

The interaction between aerodynamic, inertial and elastic forces results in a complex fluid-solid interaction (FSI). Thus, to improve the design process and control of such structures, the exact determination of induced loads in the presence of aeroelastic considerations is necessary. For this purpose, numerical and experimental techniques are used. However, the experimental methods may face the problem in simultaneous measurement of plate deformations, aerodynamic force, and plate kinematics. To overcome these difficulties, numerical methods or simulations are more attractive.

3.2 Summary of Works in the Current Study

The purpose of the current study was to characterize the dynamic stability of rectangular plates subjected to parallel supersonic flow. The solid model used Sanders' shell theory. The quadrilateral finite element shape functions are two-dimensional polynomial functions of order three for transverse displacement and of order two for the in-plane displacements. The solid model is coupled with first order piston theory to account for aerodynamic pressure. Calculations were performed for plates with various geometrical properties and boundary conditions. Two kinds of dynamic instability were found in our results: the coupled-mode flutter and divergence. Cantilevered plates may lose their stability first through divergence and then by flutter due to coupling of the first and second modes. The results obtained using the present model were validated by comparing them to the existing works in the literature and a very good agreement was observed. This approach makes it possible to model plates with mechanical properties varying from one point to another in the structure or having geometric discontinuities.

CHAPTER 4 CONCLUSION AND RECOMMENDATIONS

A numerical investigation for solid model coupled with fluid for an isotropic rectangular platehas been carried out for various geometrical properties and boundary conditions. The following observations were made:

- By increasing the thickness ratio, the critical non-dimensional aerodynamic pressure (λ_{cr}) was increased for all boundary conditions.
- By increasing the geometrical ratio (A/B), the critical non-dimensional aerodynamic pressure (λ_{cr}) was increased for case 1 (SSSS), case 3 (CFCF), case 5 (CFFF) and case 7 (SFSS) and decreased for case 2 (FCFC) and case 4 (FFFC).
- By increasing the geometrical ratio (A/B), the critical non-dimensional aerodynamic pressure (λ_{cr}) was increased first and then was decreased for case 6 (FCFF).
- In case 7 (SFSS) and case 4 (FFFC), for all geometrical properties and boundary conditions, we had divergence.
- In case 1 (SSSS), case 2 (FCFC), case 5 (CFFF) and case 6 (FCFF) for all geometrical properties and boundary conditions, we had flutter.
- In case 3 (CFCF), for a square plate, by changing the thickness of the plate, we had only divergence. However, for a fixed thickness if A≤B we have divergence and if A>B we had flutter.

4.1 Future Research

Future works could focus on the following subjects:

- Introducing both structural and aerodynamics nonlinearities in the aeroelastic analysis of plates subjected to supersonic flow particularly in wings with high aspect ratios where large deflections are expected
- Expanding the current model to handle trapezoidal plates
- Performing analysis using anisotropic materials

- Aeroelastic analysis of isotropic and anisotropic notched plates

REFERENCES

[1] Dowell, E.H., et al., A modern course in aeroelasticity. Vol. 3. 1989: Springer.

[2] Hodges, D.H. and G.A. Pierce, Introduction to structural dynamics and aeroelasticity. Vol. 15. 2011: cambridge university press.

[3] Vlasov VZ (1951), Basic differential equations in the general theory of elastic shells, NACA TM 1241.

[4] Stroud WJ (1963), Elastic constants for bending and twisting of corrugation-stIffened panels, NASA TR-R-166.

[5] Dowell EH (1966) Nonlinear oscillations of a fluttering plate I. AIAA J 4(7):1267–1275

[6] Dowell EH (1967) Nonlinear oscillations of a fluttering plate II. AIAA J 5(10):1856–1862

[7] Olson MD (1967), Finite elements applied to panel flutter, AIAA J 5, 2267-2270.

[8] Librescu L and Malaiu E (1968), Supersonic flutter of circular cylindrical heterogeneous orthotropic thin panels of finite length, J Sound Vib 8(3), 494-512.

[9] Dixon SC and Hudson ML (1969), Flutter boundary for simply supported unstiffened cylinders, AIAA J, 7(7), 1390-1391.

[10] Olson MD (1970), Some flutter solutions using finite elements, AIAA J 8, 747-752.

[11] Erickson LL, Supersonic flutter of sandwich panels; effect of face bending stiffness, rotary inertia, and orthotropic core shear stiffnesses (1971), NASA TND-6427.

[12] Leissa AW (1973), Vibration of shells, NASA SP-288.

[13] Bismarck-Nasr MN (1977), Finite element method applied to the flutter of two parallel elastically coupled flat plates, Int J Num Meth Engng 11, 1188-1193.

[14] Singa Rao K and Venkateswara Rao G (1983), Nonlinear supersonic flutter of panels considering shear deformation and rotary inertia, Int J Compt and Str'll.et 17(3), 361-364.

[15] Chen WH and Lin HC (1985), Flutter analysis of thin cracked panels using the finite element method, AIAA J. 23(5), 795-801.

[16] Sarma BS and Varadan TK (1988), Nonlinear panel flutter by finite-element method, AIAA .126(5), 566-574.

[17] Lin KJ, Lu PJ, and Tarn JQ (1989), Flutter analysis of composite panels using high-precision finite elements, Int J Compt and Struct 33(2), 561-574.

[18] Lock, M. H. and Fung, Y. C., "Comparative Experimental and Theoretical Studies of the Flutter of Flat Panels in a Low Supersonic Flow," AFOSR TN 670, May 1961, Guggenheim Aeronautical Lab., California Institute of Technology, Pasadena, Calif.

[19] Hess, R. W. and Gibson, F. W., "Experimental Investigation of the Effects of Compressive Stress on the Flutter of a Curved Panel and a Flat Panel at Supersonic Mach Numbers," TN D-1386, Oct. 1962, NASA.

[20] Dowell, E. H. and Voss, H. M., "Experimental and Theoretical Panel Flutter Studies in the Mach Number Range 1.0 to 5.0," TDR 63-449, Dec. 1963, Aeronautical Systems Division,. United States Air Force; also AIAA Journal, Vol. 3, No. 12, Dec. 1965, pp. 2292 2304.

[21] Shideler, J. L., Dixon, S. C., and Shore, C. P., "Flutter at Mach 3 Thermally Stressed Panels and Comparison with Theory for Panels with Edge Rotational Restraint," TN D-3498, Aug. 1966, NASA.

[22] Muhlstein, L., Jr., Gaspers, P. A., Jr., and Riddle, D. W., "An Experimental Study of the Influence of the Turbulent Boundary Layer on Panel Flutter," TN D-4486, 1968, NASA.

[23] Dowell, E. H., "Theoretical-Experimental Correlation of Plate Flutter Boundaries at Low Supersonic Speeds," AIAA Journal, Vol. 6, No. 9, Sept. 1969, pp. 1810-1811.

[24] Bismarck-Nasr MN, "Finite element analysis of aeroelasticity of plates and shells," Appl Mech Rev vol 45, no 12, part 1, December 1992

[25] Laith K. Abbas · Xiaoting Rui · P. Marzocca, "Panel flutter analysis of plate element based on the absolute nodal coordinate formulation", Journal of Multibody System Dynamics, July 2011, p. 135–152.

[26] Elizabeth M. Bloomhardt, Earl H. Dowell, "A Study of the Aeroelastic Behavior of Flat Plates and Membranes with Mixed Boundary Conditions in Axial Subsonic Flow", 52nd AIAA/ASME/ASCE/AHS/ASC Structures, Structural Dynamics and Materials Conference
 19th 4 - 7 April 2011, Denver, Colorado

[27] Dan Xie, Min Xu, Earl H.Dowell, "Projection-free proper orthogonal decomposition method for a cantilever plate in supersonic flow", Journal of Sound and Vibration, 333 (2014) p. 6190–6208.

[28] S. Chad Gibbs, Ivan Wang, Earl H. Dowell, "Stability of Rectangular Plates in Subsonic Flow with Various Boundary Conditions", Journal of Aircraft, Vol. 52, No. 2, March–April 2015.

[29] Kerboua, Y., et al., "Vibration analysis of rectangular plates coupled with fluid", Applied Mathematical Modelling, 2008. 32(12): p. 2570-2586.

[30] Katsikadelis, J. and N. Babouskos, "Nonlinear flutter instability of thin damped plates: A solution by the analog equation method", Journal of Mechanics of Materials and structures, 2009. 4(7): p. 1395-1414.

[31] Song, Z.-G. and F.-M. Li, "Investigations on the flutter properties of supersonic panels with different boundary conditions. International Journal of Dynamics and Control", 2014. 2(3): p. 346-353.

[32] Dowell, E. and W. Ye, Limit cycle oscillation of a fluttering cantilever plate. AIAA journal, 1991. 29(11): p. 1929-1936.

[33] Xie, D., et al., "Observation and evolution of chaos for a cantilever plate in supersonic flow", Journal of Fluids and Structures, 2014. 50: p. 271-291.

[34] Xie, D. and M. Xu, "A comparison of numerical and semi-analytical proper orthogonal decomposition methods for a fluttering plate", Journal of Nonlinear Dynamics, 2015. 79(3): p. 1971-1989.

[35] Mahran, M., H. Negm, and A. El-Sabbagh, "Aero-elastic characteristics of tapered plate wings. Finite Elements in Analysis and Design", 2015. 94: p. 24-32.

[36] Ganji, H.F. and E.H. Dowell, "Panel flutter prediction in two dimensional flow with enhanced piston theory. Journal of Fluids and Structures", 2016. 63: p. 97-102.

[37] Dowell, E.H. and H.F. Ganji, "Investigation of higher order effects in linear piston theory", Mathematics in Engineering, Science & Aerospace (MESA), 2016. 7(1).

[38] Tian, W., et al., "Analysis of nonlinear aeroelastic characteristics of a trapezoidal wing in hypersonic flow", Journal of Nonlinear Dynamics, 2017. 89(2): p. 1205-1232.

[39] Aravinth, D., et al. "Dynamic Aeroelasticity of a Trapezoidal Wing Using Enhanced Piston Theory", 2018, AIAA/ASCE/AHS/ASC Structures, Structural Dynamics, and Materials Conference.

[40] Lin, H., et al., "Studies for aeroelastic characteristics and nonlinear response of FG-CNT reinforced composite panel considering the transient heat conduction", Journal of Composite Structures, 2018. 188: p. 470-482.

[41] AA Lakis, MP Paidoussis, "Dynamic analysis of axially non-uniform thin cylindrical shells", Journal of Mechanical Engineering Science, vol 14, Feb. 1972, pp. 49-71.

[42] A Selmane, AA Lakis, "Non-linear dynamic analysis of orthotropic open cylindrical shells subjected to a flowing fluid", Journal of Sound and Vibration, vol 202, April 1997, pp. 67-93.

APPENDIX A

A1.Elements of elasticity matrix for an isotropic material:

$$P = \begin{bmatrix} D & \nu D & 0 & 0 & 0 & 0 \\ \nu D & D & 0 & 0 & 0 & 0 \\ 0 & 0 & (1-\nu)D/2 & 0 & 0 & 0 \\ 0 & 0 & 0 & K & \nu K & 0 \\ 0 & 0 & 0 & \nu K & K & 0 \\ 0 & 0 & 0 & 0 & 0 & (1-\nu)K/2 \end{bmatrix}$$

In the above matrix, $D = Eh/1-\nu^2$ and $K = Eh^3/12(1-\nu^2)$

APPENDIX B

B1. Elements of matrix R

$$R = \begin{bmatrix} 1 & \frac{x}{A} & \frac{y}{B} & \frac{xy}{AB} & 0 & 0 & 0 & 0 & 0 & 0 & 0 & 0 & 0 & 0 & 0 & 0 & 0 & 0 & 0 & 0 & 0 & 0 & 0 & 0 & 0 \\ 0 & 0 & 0 & 0 & 1 & \frac{x}{A} & \frac{y}{B} & \frac{xy}{AB} & 0 & 0 & 0 & 0 & 0 & 0 & 0 & 0 & 0 & 0 & 0 & 0 & 0 & 0 & 0 & 0 & 0 \\ 0 & 0 & 0 & 0 & 0 & 0 & 0 & 0 & 1 & \frac{x}{A} & \frac{y}{B} & \frac{x^2}{2A^2} & \frac{xy}{AB} & \frac{y^2}{2B^2} & \frac{x^3}{6A^3} & \frac{x^2y}{2A^2B} & \frac{xy^2}{2AB^2} & \frac{y^3}{6B^3} & \frac{x^3y}{6A^3B} & \frac{x^2y^2}{4A^2B^2} & \frac{xy^3}{6AB^3} & \frac{x^3y^2}{12A^3B^2} & \frac{x^2y^3}{12A^2B^3} & \frac{x^3y^3}{36A^3B^3} \end{bmatrix}$$

B2. Elements of matrix Q

$$Q = \begin{bmatrix} \frac{1}{A} & 0 & 0 & \frac{y}{AB} & 0 & 0 & 0 & 0 & 0 & 0 & 0 & 0 & 0 & 0 & 0 & 0 & 0 & 0 & 0 & 0 & 0 & 0 & 0 & 0 & 0 \\ 0 & 0 & 0 & 0 & 0 & 0 & \frac{1}{B} & \frac{x}{AB} & 0 & 0 & 0 & 0 & 0 & 0 & 0 & 0 & 0 & 0 & 0 & 0 & 0 & 0 & 0 & 0 & 0 \\ 0 & 0 & \frac{1}{B} & \frac{x}{AB} & 0 & \frac{1}{A} & 0 & \frac{y}{AB} & 0 & 0 & 0 & 0 & 0 & 0 & 0 & 0 & 0 & 0 & 0 & 0 & 0 & 0 & 0 & 0 & 0 \\ 0 & 0 & 0 & 0 & 0 & 0 & 0 & 0 & 0 & 0 & 0 & \frac{-1}{A^2} & 0 & 0 & \frac{-x}{A^3} & \frac{-y}{A^2B} & 0 & 0 & \frac{-xy}{A^3B} & \frac{-y^2}{2A^2B^2} & 0 & \frac{-xy^2}{2A^3B^2} & \frac{-y^3}{6A^2B^3} & \frac{-xy^3}{6A^3B^3} \\ 0 & 0 & 0 & 0 & 0 & 0 & 0 & 0 & 0 & 0 & 0 & 0 & \frac{-1}{B^2} & 0 & 0 & \frac{-x}{AB^2} & \frac{-y}{B^3} & 0 & \frac{-x^2}{2A^2B^2} & \frac{-xy}{AB^3} & \frac{-x^3}{6A^3B^2} & \frac{-x^2y}{2A^2B^3} & \frac{-x^3y}{6A^3B^3} \\ 0 & 0 & 0 & 0 & 0 & 0 & 0 & 0 & 0 & 0 & 0 & 0 & \frac{-2}{AB} & 0 & 0 & \frac{-2x}{A^2B} & \frac{-2y}{AB^2} & 0 & \frac{-x^2}{A^3B} & \frac{-2xy}{A^2B^2} & \frac{-y^2}{AB^3} & \frac{-x^2y}{A^3B^2} & \frac{-xy^2}{A^2B^3} & \frac{-x^2y^2}{2A^3B^3} \end{bmatrix}$$

B3. Elements of matrix A^{-1}

$$
\begin{bmatrix}
1 & 0 & 0 & 0 & 0 & 0 & 0 & 0 & 0 & 0 & 0 & 0 & 0 & 0 & 0 & 0 & 0 & 0 & 0 & 0 & 0 & 0 & 0 & 0 \\
\frac{-A}{x_e} & 0 & 0 & 0 & 0 & 0 & \frac{A}{x_e} & 0 & 0 & 0 & 0 & 0 & 0 & 0 & 0 & 0 & 0 & 0 & 0 & 0 & 0 & 0 & 0 & 0 \\
\frac{-B}{y_e} & 0 & 0 & 0 & 0 & 0 & 0 & 0 & 0 & 0 & 0 & 0 & 0 & 0 & 0 & 0 & 0 & 0 & 0 & \frac{B}{y_e} & 0 & 0 & 0 & 0 \\
\frac{AB}{x_e y_e} & 0 & 0 & 0 & 0 & 0 & -\frac{AB}{x_e y_e} & 0 & 0 & 0 & 0 & 0 & \frac{AB}{x_e y_e} & 0 & 0 & 0 & 0 & 0 & 0 & -\frac{AB}{x_e y_e} & 0 & 0 & 0 & 0 & 0 \\
0 & 1 & 0 & 0 & 0 & 0 & 0 & 0 & 0 & 0 & 0 & 0 & 0 & 0 & 0 & 0 & 0 & 0 & 0 & 0 & 0 & 0 & 0 & 0 \\
0 & \frac{-A}{x_e} & 0 & 0 & 0 & 0 & 0 & \frac{A}{x_e} & 0 & 0 & 0 & 0 & 0 & 0 & 0 & 0 & 0 & 0 & 0 & 0 & 0 & 0 & 0 & 0 \\
0 & \frac{-B}{y_e} & 0 & 0 & 0 & 0 & 0 & 0 & 0 & 0 & 0 & 0 & 0 & 0 & 0 & 0 & 0 & 0 & 0 & \frac{B}{y_e} & 0 & 0 & 0 & 0 \\
0 & \frac{AB}{x_e y_e} & 0 & 0 & 0 & 0 & 0 & \frac{-AB}{x_e y_e} & 0 & 0 & 0 & 0 & 0 & \frac{AB}{x_e y_e} & 0 & 0 & 0 & 0 & 0 & \frac{-AB}{x_e y_e} & 0 & 0 & 0 & 0 \\
0 & 0 & 1 & 0 & 0 & 0 & 0 & 0 & 0 & 0 & 0 & 0 & 0 & 0 & 0 & 0 & 0 & 0 & 0 & 0 & 0 & 0 & 0 & 0 \\
0 & 0 & 0 & A & 0 & 0 & 0 & 0 & 0 & 0 & 0 & 0 & 0 & 0 & 0 & 0 & 0 & 0 & 0 & 0 & 0 & 0 & 0 & 0 \\
0 & 0 & 0 & 0 & B & 0 & 0 & 0 & 0 & 0 & 0 & 0 & 0 & 0 & 0 & 0 & 0 & 0 & 0 & 0 & 0 & 0 & 0 & 0 \\
0 & 0 & \frac{-6A^2}{x_e^2} & \frac{-4A^2}{x_e} & 0 & 0 & 0 & \frac{6A^2}{x_e^2} & \frac{-2A^2}{x_e} & 0 & 0 & 0 & 0 & 0 & 0 & 0 & 0 & 0 & 0 & 0 & 0 & 0 & 0 & 0 \\
0 & 0 & 0 & 0 & 0 & AB & 0 & 0 & 0 & 0 & 0 & 0 & 0 & 0 & 0 & 0 & 0 & 0 & 0 & 0 & 0 & 0 & 0 & 0 \\
0 & 0 & \frac{-6B^2}{y_e^2} & 0 & \frac{-4B^2}{y_e} & 0 & 0 & 0 & 0 & 0 & 0 & 0 & 0 & 0 & 0 & 0 & 0 & 0 & 0 & 0 & \frac{6B^2}{y_e^2} & 0 & \frac{-2B^2}{y_e} & 0 \\
0 & 0 & \frac{12A^3}{x_e^3} & \frac{6A^3}{x_e^2} & 0 & 0 & 0 & \frac{-12A^3}{x_e^3} & \frac{6A^3}{x_e^2} & 0 & 0 & 0 & 0 & 0 & 0 & 0 & 0 & 0 & 0 & 0 & 0 & 0 & 0 & 0 \\
0 & 0 & 0 & 0 & \frac{-6A^2B}{x_e^2} & \frac{-4A^2B}{x_e} & 0 & 0 & 0 & \frac{6A^2B}{x_e^2} & \frac{-2A^2B}{x_e} & 0 & 0 & 0 & 0 & 0 & 0 & 0 & 0 & 0 & 0 & 0 & 0 & 0 \\
0 & 0 & 0 & \frac{-6AB^2}{y_e^2} & 0 & \frac{-4AB^2}{y_e} & 0 & 0 & 0 & 0 & 0 & 0 & 0 & 0 & 0 & 0 & 0 & 0 & 0 & 0 & 0 & \frac{6AB^2}{y_e^2} & 0 & \frac{-2AB^2}{y_e} \\
0 & 0 & \frac{12B^3}{y_e^3} & 0 & \frac{6B^3}{y_e^2} & 0 & 0 & 0 & 0 & 0 & 0 & 0 & 0 & 0 & 0 & 0 & 0 & 0 & 0 & 0 & \frac{-12B^3}{y_e^3} & 0 & \frac{6B^3}{y_e^2} & 0 \\
0 & 0 & 0 & 0 & \frac{12A^3B}{x_e^3} & \frac{6A^3B}{x_e^2} & 0 & 0 & 0 & 0 & \frac{-12A^3B}{x_e^3} & \frac{6A^3B}{x_e^2} & 0 & 0 & 0 & 0 & 0 & 0 & 0 & 0 & 0 & 0 & 0 & 0 \\
0 & 0 & \frac{36A^2B^2}{x_e^2 y_e^2} & \frac{24A^2B^2}{x_e y_e^2} & \frac{24A^2B^2}{x_e^2 y_e} & \frac{16A^2B^2}{x_e y_e} & 0 & 0 & \frac{-36A^2B^2}{x_e^2 y_e^2} & \frac{12A^2B^2}{x_e y_e^2} & \frac{-24A^2B^2}{x_e^2 y_e} & \frac{8A^2B^2}{x_e y_e} & \frac{36A^2B^2}{x_e^2 y_e^2} & \frac{-12A^2B^2}{x_e y_e^2} & \frac{-12A^2B^2}{x_e^2 y_e} & \frac{4A^2B^2}{x_e y_e} & 0 & 0 & 0 & 0 & \frac{-36A^2B^2}{x_e^2 y_e^2} & \frac{-24A^2B^2}{x_e y_e^2} & \frac{12A^2B^2}{x_e^2 y_e} & \frac{8A^2B^2}{x_e y_e} \\
0 & 0 & 0 & \frac{12AB^3}{y_e^3} & 0 & \frac{6AB^3}{y_e^2} & 0 & 0 & 0 & 0 & 0 & 0 & 0 & 0 & 0 & 0 & 0 & 0 & 0 & 0 & 0 & \frac{-12AB^3}{y_e^3} & 0 & \frac{6AB^3}{y_e^2} \\
0 & 0 & -\frac{72A^3B^2}{x_e^3 y_e^2} & -\frac{36A^3B^2}{x_e^2 y_e^2} & -\frac{48A^3B^2}{x_e^3 y_e} & -\frac{24A^3B^2}{x_e^2 y_e} & 0 & 0 & \frac{72A^3B^2}{x_e^3 y_e^2} & -\frac{36A^3B^2}{x_e^2 y_e^2} & \frac{48A^3B^2}{x_e^3 y_e} & -\frac{24A^3B^2}{x_e^2 y_e} & 0 & 0 & -\frac{72A^3B^2}{x_e^3 y_e^2} & \frac{36A^3B^2}{x_e^2 y_e^2} & \frac{24A^3B^2}{x_e^3 y_e} & \frac{12A^3B^2}{x_e^2 y_e} & 0 & 0 & \frac{72A^3B^2}{x_e^3 y_e^2} & \frac{36A^3B^2}{x_e^2 y_e^2} & \frac{24A^3B^2}{x_e^3 y_e} & \frac{12A^3B^2}{x_e^2 y_e} \\
0 & 0 & -\frac{72A^2B^3}{x_e^2 y_e^3} & -\frac{48A^2B^3}{x_e y_e^3} & -\frac{36A^2B^3}{x_e^2 y_e^2} & -\frac{24A^2B^3}{x_e y_e^2} & 0 & 0 & \frac{72A^2B^3}{x_e^2 y_e^3} & -\frac{24A^2B^3}{x_e y_e^3} & \frac{36A^2B^3}{x_e^2 y_e^2} & -\frac{12A^2B^3}{x_e y_e^2} & 0 & 0 & -\frac{72A^2B^3}{x_e^2 y_e^3} & \frac{24A^2B^3}{x_e y_e^3} & \frac{36A^2B^3}{x_e^2 y_e^2} & -\frac{12A^2B^3}{x_e y_e^2} & 0 & 0 & \frac{72A^2B^3}{x_e^2 y_e^3} & \frac{48A^2B^3}{x_e y_e^3} & -\frac{36A^2B^3}{x_e^2 y_e^2} & -\frac{24A^2B^3}{x_e y_e^2} \\
0 & 0 & \frac{144A^3B^3}{x_e^3 y_e^3} & \frac{72A^3B^3}{x_e^2 y_e^3} & \frac{72A^3B^3}{x_e^3 y_e^2} & \frac{36A^3B^3}{x_e^2 y_e^2} & 0 & 0 & -\frac{144A^3B^3}{x_e^3 y_e^3} & \frac{72A^3B^3}{x_e^2 y_e^3} & -\frac{72A^3B^3}{x_e^3 y_e^2} & \frac{36A^3B^3}{x_e^2 y_e^2} & 0 & 0 & \frac{144A^3B^3}{x_e^3 y_e^3} & -\frac{72A^3B^3}{x_e^2 y_e^3} & -\frac{72A^3B^3}{x_e^3 y_e^2} & \frac{36A^3B^3}{x_e^2 y_e^2} & 0 & 0 & -\frac{144A^3B^3}{x_e^3 y_e^3} & \frac{72A^3B^3}{x_e^2 y_e^3} & \frac{72A^3B^3}{x_e^3 y_e^2} & \frac{36A^3B^3}{x_e^2 y_e^2}
\end{bmatrix}
$$